

# Improved full one-loop corrections to $A^0 \rightarrow \tilde{f}_1 \tilde{f}_2$ and $\tilde{f}_2 \rightarrow \tilde{f}_1 A^0$

 C. Weber,<sup>\*</sup> H. Eberl,<sup>†</sup> and W. Majerotto<sup>‡</sup>
*Institut für Hochenergiephysik der Österreichischen Akademie der Wissenschaften, A-1050 Vienna, Austria*

(Received 16 August 2003; published 19 November 2003)

We calculate the *full* electroweak one-loop corrections to the decay of the *CP*-odd Higgs boson  $A^0$  into scalar fermions in the minimal supersymmetric extension of the standard model (MSSM). For this purpose many parameters of the MSSM have to be properly renormalized in the on-shell renormalization scheme. We have also included the supersymmetric QCD corrections. For the decay into bottom squarks and tau sleptons, especially for large  $\tan\beta$ , the corrections can be very large, making the perturbation expansion unreliable. We solve this problem by an appropriate definition of the tree-level coupling in terms of running fermion masses and running trilinear couplings  $A_f$ . We also discuss the decay of heavy scalar fermions into light scalar fermions and  $A^0$ . We find that the corrections can be sizable and therefore cannot be neglected.

DOI: 10.1103/PhysRevD.68.093011

PACS number(s): 12.15.Lk, 12.60.Jv, 14.80.Cp

## I. INTRODUCTION

The search for a Higgs boson is the primary goal of all present and future high energy experiments at the Fermilab Tevatron, CERN Large Hadron Collider (LHC) or an  $e^+e^-$  Linear Collider. Whereas the standard model (SM) predicts just one Higgs boson, with the present lower bound of its mass  $m_H \geq 114.4$  GeV (at 95% confidence level) [1], extensions of the SM allow for more Higgs bosons. In particular, the minimal supersymmetric standard model (MSSM) contains five physical Higgs bosons: two neutral *CP*-even ( $h^0$  and  $H^0$ ), one neutral *CP*-odd ( $A^0$ ), and two charged ones ( $H^\pm$ ) [2,3]. The existence of a charged Higgs boson or a *CP*-odd neutral one would give clear evidence for physics beyond the SM. For a discovery precise predictions for its decay modes and their branching ratios are necessary. If supersymmetric (SUSY) particles are not too heavy, the Higgs bosons can also decay into SUSY particles (neutralinos  $\tilde{\chi}_i^0$ , charginos  $\tilde{\chi}_k^\pm$ , sfermions  $\tilde{f}_m$ ),  $H^0, A^0 \rightarrow \tilde{\chi}_i^0 \tilde{\chi}_j^0$  ( $i, j = 1, \dots, 4$ ),  $H^0, A^0 \rightarrow \tilde{\chi}_k^+ \tilde{\chi}_l^-$  ( $k, l = 1, 2$ ),  $H^0, A^0 \rightarrow \tilde{f}_m \tilde{f}_n$  ( $m, n = 1, 2$ ),  $H^\pm \rightarrow \tilde{\chi}_k^+ \tilde{\chi}_i^0$ ,  $H^\pm \rightarrow \tilde{f}_m \tilde{f}'_n$ . At the tree level, these decays were studied in [4,5]. In particular, the branching ratios for the decays into sfermions,  $H^0, A^0 \rightarrow \tilde{f}_m \tilde{f}_n$ , can be sizable depending on the parameter space [6,7]. The SUSY QCD corrections to the decays into sfermions have also been calculated [8,9]. The corrections to the decays into neutralinos [10] or charginos [11] due to fermion/sfermion exchanges have also been found non-negligible.

In this paper, we study in detail the decay of the *CP*-odd Higgs boson  $A^0$  into two sfermions,  $A^0 \rightarrow \tilde{f}_1 \tilde{f}_2$ . In particular, the third generation sfermions  $\tilde{t}_i, \tilde{b}_i$ , and  $\tilde{\tau}_i$  are interesting because one expects them to be lighter than the other sfer-

mions due to their large Yukawa couplings and left-right mixings. Since  $A^0$  couples only to  $\tilde{f}_L \tilde{f}_R$  (left-right states of  $\tilde{f}$ ), and due to the *CP* nature of  $A^0$ ,  $A^0 \rightarrow \tilde{f}_i \tilde{f}_i$  vanishes. (This is valid also beyond the tree level for real parameters in the MSSM.) We will calculate the *full* electroweak corrections in the on-shell scheme. Owing to the fact that almost all parameters of the MSSM have to be renormalized in this process and hence a large number of graphs has to be computed, the calculation is very complex. Despite this complexity, we have performed the calculation in an analytic way. We have also studied the crossed channel  $\tilde{f}_2 \rightarrow \tilde{f}_1 A^0$ . Some important numerical results, especially for the decays of  $A^0$  into the third generation squarks and the corresponding crossed channels, have already been shown in [12].

This paper has three new elements. First, we give in the Appendixes all analytical formulas needed for the calculation. Second, we describe in detail our method for improving the full one-loop calculation. As pointed out in [12], in the case of the decay of  $A^0 \rightarrow \tilde{b}_1 \tilde{b}_2$  or  $A^0 \rightarrow \tilde{\tau}_1 \tilde{\tau}_2$  the decay widths can receive large corrections, especially for large  $\tan\beta$ . This makes the perturbation expansion unreliable. In some cases the width can even become negative in the on-shell renormalization scheme. We present here a detailed description of how this problem can be solved by an appropriate definition of the tree-level coupling in terms of running fermion masses and running trilinear coupling  $A_f$  ( $f = b, \tau$ ). For consistency between the on-shell and the dimensional reduction (DR) running parameters an iteration procedure is necessary. Moreover, in addition to the numerical results shown in [12] we present here new results for  $A^0 \rightarrow \tilde{t}_1 \tilde{t}_2$ ,  $A^0 \rightarrow \tilde{b}_1 \tilde{b}_2$ ,  $A^0 \rightarrow \tilde{\tau}_1 \tilde{\tau}_2$  and the corresponding crossed channels.

The paper is organized as follows. In Sec. II we summarize the tree-level formulas. In Sec. III the full electroweak corrections are presented for which the explicit analytic formulas are given in Appendixes B, C, and D. In Sec. IV a detailed description of the method to improve the one-loop calculation is presented. In Sec. V the numerical treatment as

<sup>\*</sup>Electronic address: weber@hephy.oeaw.ac.at

<sup>†</sup>Electronic address: helmut@hephy.oeaw.ac.at

<sup>‡</sup>Electronic address: majer@hephy.oeaw.ac.at

well as numerical results are shown. Section VI summarizes our conclusions.

## II. TREE-LEVEL RESULT

The sfermion mixing is described by the sfermion mass matrix in the left-right basis  $(\tilde{f}_L, \tilde{f}_R)$ , and in the mass basis  $(\tilde{f}_1, \tilde{f}_2)$ ,  $\tilde{f} = \tilde{t}, \tilde{b}$  or  $\tilde{\tau}$ ,

$$\mathcal{M}_{\tilde{f}}^2 = \begin{pmatrix} m_{\tilde{f}_L}^2 & a_f m_f \\ a_f m_f & m_{\tilde{f}_R}^2 \end{pmatrix} = (R^{\tilde{f}})^\dagger \begin{pmatrix} m_{\tilde{f}_1}^2 & 0 \\ 0 & m_{\tilde{f}_2}^2 \end{pmatrix} R^{\tilde{f}}, \quad (2.1)$$

where  $R_{i\alpha}^{\tilde{f}}$  is a  $2 \times 2$  rotation matrix with rotation angle  $\theta_{\tilde{f}}$ , which relates the mass eigenstates  $\tilde{f}_i$ ,  $i = 1, 2$  ( $m_{\tilde{f}_1} < m_{\tilde{f}_2}$ ), to the gauge eigenstates  $\tilde{f}_\alpha$ ,  $\alpha = L, R$ , by  $\tilde{f}_i = R_{i\alpha}^{\tilde{f}} \tilde{f}_\alpha$  and

$$m_{\tilde{f}_L}^2 = M_{\{\tilde{Q}, \tilde{L}\}}^2 + (I_f^{3L} - e_f \sin^2 \theta_W) \cos 2\beta m_Z^2 + m_f^2, \quad (2.2)$$

$$m_{\tilde{f}_R}^2 = M_{\{\tilde{U}, \tilde{D}, \tilde{E}\}}^2 + e_f \sin^2 \theta_W \cos 2\beta m_Z^2 + m_f^2, \quad (2.3)$$

$$a_f = A_f - \mu (\tan \beta)^{-2I_f^{3L}}. \quad (2.4)$$

$M_{\tilde{Q}}$ ,  $M_{\tilde{L}}$ ,  $M_{\tilde{U}}$ ,  $M_{\tilde{D}}$  and  $M_{\tilde{E}}$  are soft SUSY breaking masses,  $A_f$  is the trilinear scalar coupling parameter,  $\mu$  is the Higgsino mass parameter,  $\tan \beta = v_2/v_1$  is the ratio of the vacuum expectation values of the two neutral Higgs doublet states [2,3],  $I_f^{3L}$  denotes the third component of the weak isospin of the fermion  $f$ ,  $e_f$  is the electric charge in terms of the elementary charge  $e_0$ , and  $\theta_W$  is the Weinberg angle.

The mass eigenvalues and the mixing angle in terms of primary parameters are

$$m_{\tilde{f}_{1,2}}^2 = \frac{1}{2} (m_{\tilde{f}_L}^2 + m_{\tilde{f}_R}^2 \mp \sqrt{(m_{\tilde{f}_L}^2 - m_{\tilde{f}_R}^2)^2 + 4a_f^2 m_f^2}), \quad (2.5)$$

$$\cos \theta_{\tilde{f}} = \frac{-a_f m_f}{\sqrt{(m_{\tilde{f}_L}^2 - m_{\tilde{f}_R}^2)^2 + 4a_f^2 m_f^2}} \quad (0 \leq \theta_{\tilde{f}} < \pi), \quad (2.6)$$

and the trilinear breaking parameter  $A_f$  can be written as

$$m_f A_f = m_{LR}^2 + m_f \mu (\tan \beta)^{-2I_f^{3L}} \quad (2.7)$$

with  $m_{LR}^2 \equiv (m_{\tilde{f}_1}^2 - m_{\tilde{f}_2}^2) \sin \theta_{\tilde{f}} \cos \theta_{\tilde{f}}$ .

At the tree level the decay width of  $A^0 \rightarrow \tilde{f}_1 \tilde{f}_2^*$  is given by

$$\Gamma^{\text{tree}}(A^0 \rightarrow \tilde{f}_1 \tilde{f}_2^*) = \frac{N_C^f \kappa(m_{A^0}^2, m_{\tilde{f}_1}^2, m_{\tilde{f}_2}^2)}{16\pi m_{A^0}^3} |G_{123}^{\tilde{f}}|^2 \quad (2.8)$$

with  $\kappa(x, y, z) = \sqrt{(x-y-z)^2 - 4yz}$  and the color factor  $N_C^f = 3$  for squarks and  $N_C^f = 1$  for sleptons, respectively.  $G_{ij3}^{\tilde{f}}$  denotes the  $A^0 \tilde{f}_i^* \tilde{f}_j$  coupling as given in Appendix A.

## III. FULL ELECTROWEAK CORRECTIONS

The full one-loop corrected decay width is given by

$$\Gamma(A^0 \rightarrow \tilde{f}_1 \tilde{f}_2^*) = \frac{N_C^f \kappa(m_{A^0}^2, m_{\tilde{f}_1}^2, m_{\tilde{f}_2}^2)}{16\pi m_{A^0}^3} \times [ |G_{123}^{\tilde{f}}|^2 + 2 \Re(G_{123}^{\tilde{f}} \cdot \Delta G_{123}^{\tilde{f}}) ]. \quad (3.1)$$

The (UV finite) corrections  $\Delta G_{123}^{\tilde{f}}$  consist of the vertex corrections  $\delta G_{123}^{\tilde{f}(v)}$  (Fig. 12 below), wave-function corrections and the coupling counterterm corrections  $\delta G_{123}^{\tilde{f}(c)}$  owing to the shift from the bare to the on-shell values,

$$\Delta G_{123}^{\tilde{f}} = \delta G_{123}^{\tilde{f}(v)} + \delta G_{123}^{\tilde{f}(w)} + \delta G_{123}^{\tilde{f}(c)}. \quad (3.2)$$

The renormalization procedure with the fixing of the counterterms is given in [12]. The explicit formulas for the vertex corrections  $\delta G_{123}^{\tilde{f}(v)}$  as well as the various contributions to the wave-function corrections  $\delta G_{123}^{\tilde{f}(w)}$ ,

$$\delta G_{123}^{\tilde{f}(w)} = \frac{1}{2} \Re[ \delta Z_{11}^{\tilde{f}} + \delta Z_{22}^{\tilde{f}} + \delta Z_{33}^H ] G_{123}^{\tilde{f}}, \quad (3.3)$$

can be found in Appendixes B and C. For the explicit formulas for the self-energies needed for the calculation of the counterterm correction,  $\delta G_{123}^{\tilde{f}(c)}$  [see Eq. (23) of [12]], we refer to Appendix D.

Due to the diagrams with photon exchange we also have to consider real photon emission corrections to cancel the infrared divergences (Fig. 12). Therefore the corrected (UV- and IR-convergent) decay width is

$$\Gamma^{\text{corr}}(A^0 \rightarrow \tilde{f}_1 \tilde{f}_2^*) \equiv \Gamma(A^0 \rightarrow \tilde{f}_1 \tilde{f}_2^*) + \Gamma(A^0 \rightarrow \tilde{f}_1 \tilde{f}_2^* \gamma). \quad (3.4)$$

Throughout the paper we use the SUSY invariant dimensional reduction as regularization scheme. For convenience we perform the calculation in the 't Hooft-Feynman gauge,  $\xi = 1$ .

## IV. IMPROVEMENT OF ONE-LOOP CORRECTIONS

It has already been pointed out in [12] that in the case of bottom squarks and tau sleptons, especially for large  $\tan \beta$ , the corrections to the decay widths  $A^0 \rightarrow \tilde{b}_1 \tilde{b}_2^*$  and  $A^0 \rightarrow \tilde{\tau}_1 \tilde{\tau}_2^*$  can be very large in the on-shell renormalization scheme. If the corrections are negative, the one-loop corrected width can even become negative and therefore unphysical. Hence the perturbation expansion around the on-shell tree level is no longer reliable. It has been shown in [13,14] that, in the case of decays into bottom squarks, the source of these large corrections is mainly the counterterms for  $m_b$  and the trilinear coupling  $A_b$ , in particular the SUSY QCD corrections. However, despite the absence of strong interactions for the decay into tau sleptons, the corrections become extremely large. We show that this problem can be

solved by defining an appropriate tree level in terms of running values for  $m_f$  and  $A_f$ . The expansion around this new tree level then no longer suffers from bad convergence.

### A. Correction to $m_b$

First we review the improvement of the perturbation expansion by using  $\overline{\text{DR}}$  running bottom quark masses, following [14–16].

If the Yukawa coupling  $h_b$  is given at the tree level in terms of the pole mass  $m_b$ , the one-loop corrections become very large due to gluon and gluino exchange contributions to

the counterterm  $\delta m_b$ . The large counterterm caused by the gluon loop is absorbed by using SM 2-loop renormalization group equations in the modified minimal subtraction ( $\overline{\text{MS}}$ ) scheme [14–16]. Thus we obtain the SM running bottom quark mass  $\hat{m}_b(Q)_{\text{SM}}$ :

$$\hat{m}_b(Q)_{\text{SM}}^{\overline{\text{MS}}} = \left( \frac{\hat{m}_b(Q)_{\text{SM}}^{\overline{\text{MS}}}}{\hat{m}_b(m_b)_{\text{SM}}^{\overline{\text{MS}}}} \right) \hat{m}_b(m_b)_{\text{SM}}^{\overline{\text{MS}}}. \quad (4.1)$$

The ratio  $[\hat{m}_b(Q)_{\text{SM}}^{\overline{\text{MS}}}/\hat{m}_b(m_b)_{\text{SM}}^{\overline{\text{MS}}}]$  can be expressed as

$$\frac{\hat{m}_b(Q)_{\text{SM}}^{\overline{\text{MS}}}}{\hat{m}_b(m_b)_{\text{SM}}^{\overline{\text{MS}}}} = \begin{cases} \frac{c_5(\alpha_s^{(2)}(Q)/\pi)}{c_5(\alpha_s^{(2)}(m_b)/\pi)} & (m_b < Q \leq m_t), \\ \frac{c_6(\alpha_s^{(2)}(Q)/\pi)}{c_6(\alpha_s^{(2)}(m_t)/\pi)} \frac{c_5(\alpha_s^{(2)}(m_t)/\pi)}{c_5(\alpha_s^{(2)}(m_b)/\pi)} & (Q > m_t), \end{cases}$$

where we have used the functions

$$c_5(x) = \left( \frac{23}{6} x \right)^{12/23} (1 + 1.175x) \quad (m_b < Q \leq m_t),$$

$$c_6(x) = \left( \frac{7}{2} x \right)^{4/7} (1 + 1.398x) \quad (Q > m_t),$$

and the 2-loop renormalization group equations for  $\alpha_s$  [16],

$$\alpha_s^{(2)}(Q) = \frac{12\pi}{(33 - 2n_f) \ln(Q^2/\Lambda_{n_f}^2)} \times \left( 1 - \frac{6(153 - 19n_f)}{(33 - 2n_f)^2} \frac{\ln \ln(Q^2/\Lambda_{n_f}^2)}{\ln(Q^2/\Lambda_{n_f}^2)} \right), \quad (4.2)$$

with  $n_f = 5$  or 6 for  $m_b < Q \leq m_t$  or  $Q > m_t$ , respectively. For the SM  $\overline{\text{DR}}$  running bottom quark mass at the scale  $Q = m_b$  we use the  $\overline{\text{MS}}$  equation

$$\hat{m}_b(m_b)_{\text{SM}}^{\overline{\text{MS}}} = m_b \left[ 1 + \frac{4}{3} \frac{\alpha_s^{(2)}(m_b)}{\pi} + K_q \left( \frac{\alpha_s^{(2)}(m_b)}{\pi} \right)^2 \right]^{-1} \quad (4.3)$$

with  $K_q = 12.4$  and then convert to  $\overline{\text{DR}}$  using one-loop running  $\alpha_s(Q)$ :

$$\hat{m}_b(Q)_{\text{SM}} = \left( \frac{\hat{m}_b(Q)_{\text{SM}}^{\overline{\text{MS}}}}{\hat{m}_b(m_b)_{\text{SM}}^{\overline{\text{MS}}}} \right) \hat{m}_b(m_b)_{\text{SM}}^{\overline{\text{MS}}} - \frac{\alpha_s(Q)}{3\pi} m_b. \quad (4.4)$$

In the MSSM, for large  $\tan \beta$  the counterterm to  $m_b$  can be very large due to the gluino-mediated graph [13,17,18]. Here we absorb the gluino contribution as well as the sizable contributions from neutralino and chargino loops and the remaining electroweak self-energies into the Higgs-boson-sfermion-sfermion tree-level coupling. In this way we obtain the full  $\overline{\text{DR}}$  running bottom quark mass

$$\hat{m}_b(Q)_{\text{MSSM}} = \hat{m}_b(Q)_{\text{SM}} + \delta m_b(Q). \quad (4.5)$$

The explicit form of the electroweak contribution to the counterterm  $\delta m_b(Q)$  is given in Appendix D 4.

### B. Correction to $A_{b,\tau}$

The second source of a very large correction (in the on-shell scheme) is the counterterms for the trilinear coupling  $A_{b,\tau}$  [see Eq. (2.7)],

$$\delta A_{b,\tau} = \frac{\delta m_{LR}^2}{m_{b,\tau}} - \frac{m_{LR}^2}{m_{b,\tau}} \frac{\delta m_{b,\tau}}{m_{b,\tau}} + \delta \mu \tan \beta + \mu \delta \tan \beta. \quad (4.6)$$

Again, the big bottom quark mass correction  $\delta m_b$  contributes to  $\delta A_b$ , but the counterterm of the left-right mixing elements of the sfermion mass matrix,  $\delta m_{LR}^2$ , also gives a very large correction for higher values of  $\tan \beta$ . In particular, in the case of the decay into staus, this is the main source for the bad convergence of the tree-level expansion. As in the case of the large correction to  $m_b$  we redefine the Higgs-boson-sfermion-sfermion tree-level coupling in terms of  $\overline{\text{DR}}$  running  $\hat{A}_{b,\tau}(m_{A^0})$ . Because of the fact that the counterterms  $\delta A_{b,\tau}$  (for large  $\tan \beta$ ) can become several orders of magnitude larger than the on-shell  $A_{b,\tau}$  we use  $\hat{A}_{b,\tau}(m_{A^0})$  as input [14]. In order to be consistent we have to perform an itera-

tion procedure to get all the correct running and on-shell masses, mixing angles and other parameters. This procedure is described below.

## V. METHOD OF IMPROVEMENT

In this section we will explain in detail how we can improve the perturbation calculation for the bottom squark and stau cases by using  $\overline{\text{DR}}$  running values for  $m_b$  and  $A_{b,\tau}$  in the Higgs-boson-sfermion-sfermion tree-level couplings. Since we take  $\overline{\text{DR}}$  running values for  $\hat{A}_b$  and  $\hat{A}_\tau$  as input and all other parameters on shell we will have to pay attention to the bottom squark and stau sector in order to get consistently all needed running and on-shell masses, mixing angles and other parameters. Here we adopt the procedure developed in [14] and also extend it to the electroweak case.

### A. Calculation of running and on-shell parameters

#### 1. Top squark sector

We start our calculation in the top squark sector. Because all input parameters in the top squark sector are on shell we obtain the on-shell masses  $m_{\tilde{t}_1}$ ,  $m_{\tilde{t}_2}$  and the top squark mixing angle  $\theta_{\tilde{t}}$  by diagonalizing the top squark mass matrix in the  $\tilde{t}_L\text{-}\tilde{t}_R$  basis; see Sec. II. The running top squark masses  $\hat{m}_{\tilde{t}_i}$  and mixing angle  $\hat{\theta}_{\tilde{t}}$  are calculated at the scale  $Q=Q_{\tilde{t}}$   $=\sqrt{m_{\tilde{t}_1}m_{\tilde{t}_2}}$  by adding the appropriate counterterms to the on-shell values in

$$\hat{m}_{\tilde{t}_i}^2(Q_{\tilde{t}}) = m_{\tilde{t}_i}^2 + \delta m_{\tilde{t}_i}^2, \quad (5.1)$$

$$\delta m_{\tilde{t}_i}^2 = \Re \Pi_{ii}^{\tilde{t}}(m_{\tilde{t}_i}^2), \quad (5.2)$$

$$\hat{\theta}_{\tilde{t}}(Q_{\tilde{t}}) = \theta_{\tilde{t}} + \delta \theta_{\tilde{t}}. \quad (5.3)$$

The electroweak parts of the sfermion self-energies  $\Pi_{ii}^{\tilde{f}}(m_{\tilde{f}_i}^2)$  are given in Appendix D 6 and the SUSY QCD contributions  $\Pi_{ii}^{\text{SUSY QCD}}(m_{\tilde{f}_i}^2)$  are given in Eqs. (25)–(27) in [8]. Here and in the following all running parameters  $\hat{X}(Q)$  are related to their on-shell values  $X$  by  $\hat{X}(Q) = X + \delta X$ , with  $\delta X$  being the full one-loop counter term—also including the SUSY QCD parts. The mixing angle is fixed by [19]

$$\begin{aligned} \delta \theta_{\tilde{f}} &= \frac{1}{4} (\delta Z_{12}^{\tilde{f}} - \delta Z_{21}^{\tilde{f}}) \\ &= \frac{1}{2(m_{\tilde{f}_1}^2 - m_{\tilde{f}_2}^2)} \Re (\Pi_{12}^{\tilde{f}}(m_{\tilde{f}_2}^2) + \Pi_{21}^{\tilde{f}}(m_{\tilde{f}_1}^2)). \end{aligned} \quad (5.4)$$

For  $\overline{\text{DR}}$  running  $\hat{m}_t$  we use the formulas from Sec. IV A with the obvious substitutions  $m_b \rightarrow m_t$  and  $K_q = 10.9$  for the topquark-case. Next we evaluate the running parameters  $\hat{M}_{\tilde{Q}}(Q)$  and  $\hat{M}_{\tilde{U}}(Q)$  by inserting the running values

$\hat{m}_{\tilde{t}_i}^2(Q), \hat{\theta}_{\tilde{t}}(Q), \hat{m}_t(Q)_{\text{MSSM}}, \hat{m}_Z(Q) = m_Z + \delta m_Z, \hat{\beta}(Q) = \beta + \delta \beta$  and  $\hat{\theta}_W = \theta_W - (1/\sin \theta_W)(\delta m_W/m_W - \delta m_Z/m_Z)$  into the equations

$$\begin{aligned} M_{\tilde{Q}}^2 &= m_{\tilde{t}_1}^2 \cos^2 \theta_{\tilde{t}} + m_{\tilde{t}_2}^2 \sin^2 \theta_{\tilde{t}} - m_t^2 \\ &\quad - m_Z^2 \cos 2\beta (I_{\tilde{t}}^{3L} - e_t \sin^2 \theta_W), \end{aligned} \quad (5.5)$$

$$\begin{aligned} M_{\tilde{U}}^2 &= m_{\tilde{t}_1}^2 \sin^2 \theta_{\tilde{t}} + m_{\tilde{t}_2}^2 \cos^2 \theta_{\tilde{t}} - m_t^2 \\ &\quad - m_Z^2 \cos 2\beta e_t \sin^2 \theta_W. \end{aligned} \quad (5.6)$$

For the running value of  $A_t$  we use [see Eq. (2.7)]

$$\hat{A}_t = (\hat{m}_{\tilde{t}_1}^2 - \hat{m}_{\tilde{t}_2}^2) \frac{\sin 2\hat{\theta}_{\tilde{t}}}{\hat{m}_t} + \hat{\mu} \cot \hat{\beta}, \quad (5.7)$$

where we have taken the running  $\hat{\mu}(Q) = \mu + (\delta X)_{22}$  [20,21].

#### 2. Bottom squark sector

In the bottom squark sector we have given all parameters on shell except the parameter for the trilinear coupling,  $\hat{A}_b(Q)$ , which is running. First we calculate  $\hat{m}_b(Q_{\tilde{b}})_{\text{MSSM}}$  from Eq. (4.5) at the scale  $Q_{\tilde{b}} = \sqrt{m_{\tilde{b}_1}m_{\tilde{b}_2}}$ . From the top squark sector we already know the running values of  $M_{\tilde{Q}}, \tan \beta$  and  $\mu$ . Then we diagonalize the bottom squark mass matrix using  $\hat{m}_b(Q_{\tilde{b}})_{\text{MSSM}}, \hat{M}_{\tilde{Q}}, \tan \hat{\beta}, \hat{\mu}$  and on-shell  $M_{\tilde{D}}$ , which is near its running value  $\hat{M}_{\tilde{D}}$ , to obtain the starting values for  $\hat{m}_{\tilde{b}_i}$  and  $\hat{\theta}_{\tilde{b}}$ . The on-shell bottom squark masses  $m_{\tilde{b}_i}$  and the mixing angle  $\theta_{\tilde{b}}$  are calculated from their running values by subtracting the appropriate counterterms, i.e.  $m_{\tilde{b}_i}^2 = \hat{m}_{\tilde{b}_i}^2(Q) - \delta m_{\tilde{b}_i}^2$ ,  $\theta_{\tilde{b}} = \hat{\theta}_{\tilde{b}}(Q) - \delta \theta_{\tilde{b}}$ . Now we can compute the running value for  $M_{\tilde{D}}$ . Using the relation [see Eq. (2.3)]

$$M_{\tilde{D}}^2 = m_{\tilde{b}_1}^2 \sin^2 \theta_{\tilde{b}} + m_{\tilde{b}_2}^2 \cos^2 \theta_{\tilde{b}} - m_b^2 - m_Z^2 \cos 2\beta e_b \sin^2 \theta_W \quad (5.8)$$

we get  $\hat{M}_{\tilde{D}} = (M_{\tilde{D}}^2 + \delta M_{\tilde{D}}^2)^{1/2} \approx M_{\tilde{D}} + \delta M_{\tilde{D}}^2 / (2M_{\tilde{D}})$  with

$$\begin{aligned} \delta M_{\tilde{D}}^2 &= \delta m_{\tilde{b}_1}^2 \sin^2 \theta_{\tilde{b}} + \delta m_{\tilde{b}_2}^2 \cos^2 \theta_{\tilde{b}} + (m_{\tilde{b}_1}^2 - m_{\tilde{b}_2}^2) \sin 2\theta_{\tilde{b}} \delta \theta_{\tilde{b}} \\ &\quad - 2m_b \delta m_b - \delta m_Z^2 \cos 2\beta e_b \sin^2 \theta_W \\ &\quad + 2m_Z^2 \sin 2\beta \delta \beta e_b \sin^2 \theta_W - m_Z^2 \cos 2\beta e_b \delta \sin^2 \theta_W \end{aligned} \quad (5.9)$$

and  $\delta m_b = \hat{m}_b(Q_{\tilde{b}})_{\text{MSSM}} - m_b$ . Because the parameters involved in these calculations are very entangled, e.g.  $\hat{M}_{\tilde{D}}$



depends on the  $\delta m_{\tilde{b}_i}$  which themselves depend on  $M_{\tilde{D}}$ , we have to perform an iteration procedure.

### 3. Iteration procedure

Here we will describe in detail the procedure for obtaining all necessary on-shell and running parameters. For convenience, we briefly denote all masses, parameters, couplings etc. for a certain  $n \geq 1$  in the iteration by  $\hat{\mathcal{X}}^{(n)}$ . As starting values  $\hat{\mathcal{X}}^{(0)}$  we take on-shell masses and parameters (except  $\hat{A}_b$  which is running) and the couplings derived from these quantities. The only exceptions are the standard model running fermion masses  $\hat{m}_f^{(0)} = \hat{m}_f(Q)_{\text{SM}} \cdot \hat{m}_f$  stands for the full DR running fermion masses,  $\hat{m}_f(Q)_{\text{MSSM}}$ .

The single steps of the iteration procedure are the following:

(1) The running top squark masses and the top squark mixing angle are calculated as explained above by  $\hat{m}_{\tilde{t}_i}^{2(n)} = m_{\tilde{t}_i}^2 + \delta m_{\tilde{t}_i}^{2(n)}(\hat{\mathcal{X}}^{(n-1)})$  and  $\hat{\theta}_{\tilde{t}}^{(n)} = \theta_{\tilde{t}} + \delta \theta_{\tilde{t}}^{(n)}(\hat{\mathcal{X}}^{(n-1)})$ .

(2)  $\hat{m}_t^{(n)} = \hat{m}_{t,\text{SM}} + \delta m_t^{(n)}(\hat{\mathcal{X}}^{(n-1)})$ .

(3)  $\hat{m}_Z^{(n)} = m_Z + \delta m_Z^{(n)}(\hat{\mathcal{X}}^{(n-1)})$  and  $\sin^2 \hat{\theta}_W^{(n)} = \sin^2 \theta_W + \delta \sin^2 \theta_W^{(n)}$  with  $\delta \sin^2 \theta_W^{(n)} = -\cos^2 \theta_W (\delta m_W / m_W - \delta m_Z / m_Z)(\hat{\mathcal{X}}^{(n-1)})$ .

(4) The running value of  $\tan \beta$ ,  $\tan \hat{\beta}^{(n)} = \tan \beta + \delta \tan \beta^{(n)}$ , with

$$\delta \tan \beta^{(n)} = (1/m_Z \sin 2\beta) \text{Im} \Pi_{A^0 Z^0}(\hat{\mathcal{X}}^{(n-1)}) \tan \beta \quad [22].$$

(5)  $\hat{\mu}^{(n)} = \mu + \delta \mu^{(n)}$  with  $\delta \mu^{(n)} = \delta X_{22}(\hat{\mathcal{X}}^{(n-1)})$ .

(6) The soft SUSY breaking masses  $\hat{M}_{\tilde{Q}, \tilde{U}}$  are calculated from  $\hat{m}_{\tilde{t}_i}^{(n)}$ ,  $\hat{\theta}_{\tilde{t}}^{(n)}$ ,  $\hat{m}_t(Q_{\tilde{t}})^{(n)}$ ,  $\hat{m}_Z^{(n)}$ ,  $\sin^2 \hat{\theta}_W^{(n)}$  and  $\tan \hat{\beta}^{(n)}$ .

(7) We compute the running  $\hat{A}_t$  by using running values in Eq. (5.7):  $\hat{A}_t^{(n)} = (\hat{m}_{\tilde{t}_1}^{2(n)} - \hat{m}_{\tilde{t}_2}^{2(n)}) \sin 2\hat{\theta}_{\tilde{t}}^{(n)} / \hat{m}_t^{(n)} + \hat{\mu}^{(n)} \cot \hat{\beta}^{(n)}$ .

(8) In the bottom squark sector we obtain  $\delta m_b^{(n)}$  from the running values already calculated in steps 1–7, like  $\hat{m}_{\tilde{b}_i}^{(n)}$ ,  $\hat{\theta}_{\tilde{b}}^{(n)}$  or  $\hat{m}_f^{(n)}$ , and the remaining masses, couplings etc. from  $\hat{\mathcal{X}}^{(n-1)}$ .

(9)  $\hat{m}_b^{(n)} = \hat{m}_{b,\text{SM}} + \delta m_b^{(n)}$ .

(10) We obtain the running bottom squark masses,  $\hat{m}_{\tilde{b}_i}^{(n)}$ , and the mixing angle,  $\hat{\theta}_{\tilde{b}}^{(n)}$ , by solving the mass eigenvalue problem with the running values of  $\hat{M}_{\tilde{Q}}^{(n)}$ ,  $\hat{M}_{\tilde{D}}^{(n-1)}$ ,  $\hat{m}_b^{(n)}$ ,  $\hat{A}_b$ ,  $\hat{\mu}^{(n)}$  and  $\tan \hat{\beta}^{(n)}$ .

(11) The on-shell bottom squark masses  $m_{\tilde{b}_i}^{2(n)} = \hat{m}_{\tilde{b}_i}^{2(n)} - \delta m_{\tilde{b}_i}^{2(n)}(Q_{\tilde{b}}^{(n)})$  at the scale  $Q_{\tilde{b}}^{(n)} = \sqrt{\hat{m}_{\tilde{b}_1}^{(n)} \hat{m}_{\tilde{b}_2}^{(n)}}$ , and  $\theta_{\tilde{b}}^{(n)} = \hat{\theta}_{\tilde{b}}^{(n)} - \delta \theta_{\tilde{b}}^{(n)}$ .

(12)  $\delta M_{\tilde{D}}^{2(n)} = \delta m_{\tilde{b}_1}^{2(n)} \sin^2 \theta_{\tilde{b}} + \delta m_{\tilde{b}_2}^{2(n)} \cos^2 \theta_{\tilde{b}} + (m_{\tilde{b}_1}^2 - m_{\tilde{b}_2}^2) \times \sin 2\theta_{\tilde{b}} \delta \theta_{\tilde{b}}^{(n)} - 2m_b(\hat{m}_b^{(n)} - m_b) - \delta m_Z^{2(n)} \cos 2\beta e_b \sin^2 \theta_W + 2m_Z^2 \times \sin 2\beta \delta \beta^{(n)} e_b \sin^2 \theta_W - m_Z^2 \cos 2\beta e_b \delta \sin^2 \theta_W^{(n)}$ . (Remember that the values without a caret are on-shell ones.)

(13)  $\hat{M}_{\tilde{D}}^{(n)} = M_{\tilde{D}} + (1/2) \delta M_{\tilde{D}}^{2(n)} / M_{\tilde{D}}$ .

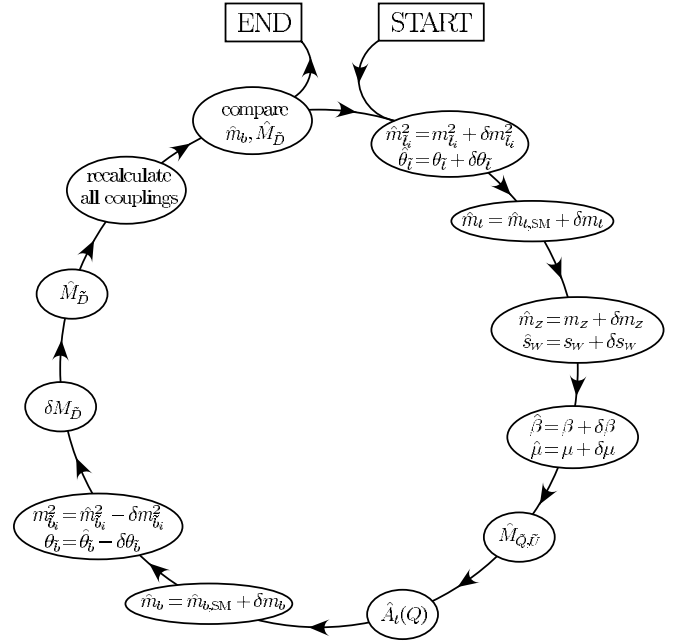


FIG. 1. Simplified flowchart for the iteration procedure. For details, see Sec. V A.

(14) In the sneutrino sector we calculate the running sneutrino mass  $\hat{m}_{\tilde{\nu}_\tau}^{2(n)} = m_{\tilde{\nu}_\tau}^2 + \delta m_{\tilde{\nu}_\tau}^{2(n)}(\hat{\mathcal{X}}^{(n-1)})$  and  $\hat{M}_{\tilde{L}}^{2(n)} = \hat{m}_{\tilde{\nu}_\tau}^{2(n)} - \frac{1}{2} \hat{m}_Z^{(n)} \cos 2\hat{\beta}^{(n)}$ ; see also Eq. (5.5).

(15) In the stau sector the values for running  $\hat{m}_\tau^{(n)}$ ,  $\hat{m}_{\tilde{\tau}_i}^{(n)}$  etc. are calculated as in steps 8–13 in the bottom squark sector with the evident substitution  $\tilde{b} \rightarrow \tilde{\tau}$  for the corresponding parameters and  $M_{\tilde{Q}} \rightarrow M_{\tilde{L}}, M_{\tilde{D}} \rightarrow M_{\tilde{E}}$ .

(16) All couplings are recalculated with the new running parameters  $\rightarrow \hat{\mathcal{X}}^n$ .

The iteration starts with  $n=1$  and ends when certain parameters are calculated precisely enough for a given accuracy, i.e.  $|1 - \hat{x}^{(n)} / \hat{x}^{(n-1)}| < \varepsilon$  for  $\hat{x} = \{\hat{m}_b, \hat{M}_{\tilde{D}}, \hat{m}_\tau, \hat{M}_{\tilde{E}}\}$ . For  $\varepsilon$  we choose  $\varepsilon = 10^{-8}$ . We have checked the consistency of this procedure by computing the on-shell  $M_{\tilde{D}}$  and running  $M_{\tilde{Q}}$  from the bottom squark sector by using

$$M_{\tilde{D}}^2 = m_{\tilde{b}_1}^2 \sin^2 \theta_{\tilde{b}} + m_{\tilde{b}_2}^2 \cos^2 \theta_{\tilde{b}} - m_b^2 - m_Z^2 \cos 2\beta e_b \sin^2 \theta_W, \quad (5.10)$$

$$\hat{M}_{\tilde{Q}}^2 = \hat{m}_{\tilde{b}_1}^2 \cos^2 \hat{\theta}_{\tilde{b}} + \hat{m}_{\tilde{b}_2}^2 \sin^2 \hat{\theta}_{\tilde{b}} - \hat{m}_b^2 - \hat{m}_Z^2 \cos 2\hat{\beta} (I_b^{3L} - e_b \sin^2 \hat{\theta}_W), \quad (5.11)$$

which are equal (up to higher order corrections) to the on-shell input  $M_{\tilde{D}}$  and running  $M_{\tilde{Q}}$  from the top squark sector.

For easier reading the single steps of the iteration procedure of the top and bottom squark sectors are depicted in the flowchart in Fig. 1.

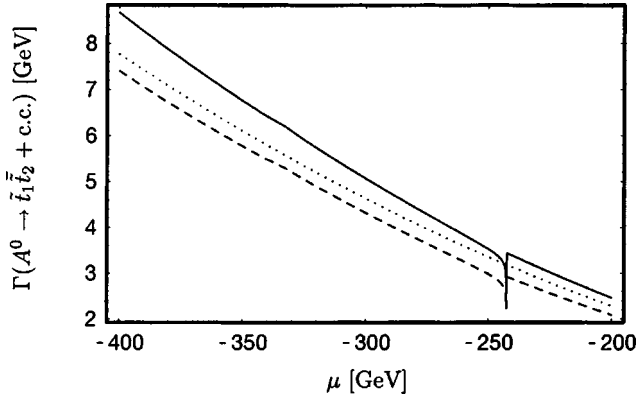


FIG. 2. Tree-level width (dotted line), full electroweak corrected decay width (dashed line) and full one-loop (electroweak and SUSY QCD) corrected width (solid line) of  $A^0 \rightarrow \tilde{t}_1 \tilde{t}_2$  as functions of  $\mu$ .

### B. Numerical results

In the following numerical examples, we take for the standard model parameters  $m_Z = 91.1876$  GeV,  $m_W = 80.423$  GeV,  $\sin^2 \theta_W = 1 - m_W^2/m_Z^2$ ,  $\alpha(m_Z) = 1/127.934$ ,  $m_t = 174.3$  GeV,  $m_b = 4.7$  GeV,  $m_\tau = 1.8$  GeV and  $\{m_u, m_d, m_e, m_c, m_s, m_\mu\} = \{4, 8, 0.511, 1300, 200, 106\}$  MeV for 1st and 2nd generation fermions.  $M'$  is fixed by the gaugino unification relation  $M' = (5/3)\tan^2 \theta_W M$ ; therefore the gluino mass is related to  $M$  by  $m_{\tilde{g}} = [\alpha_s(m_{\tilde{g}})/\alpha] \sin^2 \theta_W M$ . In order to reduce the number of parameters in the input parameter set, we assume  $M_{\tilde{Q}} \equiv M_{\tilde{Q}_3} = (10/9)M_{\tilde{U}_3} = (10/11)M_{\tilde{D}_3} = M_{\tilde{L}_3} = M_{\tilde{E}_3} = M_{\tilde{Q}_{1,2}} = M_{\tilde{U}_{1,2}} = M_{\tilde{D}_{1,2}} = M_{\tilde{L}_{1,2}} = M_{\tilde{E}_{1,2}}$  for the first, second and third generation soft SUSY breaking masses as well as  $A \equiv A_t = A_b = A_\tau$  for all (s)fermion generations, if not stated otherwise.

#### 1. Top squark case

In Fig. 2 we show the tree-level and the corrected widths to  $A^0 \rightarrow \tilde{t}_1 \tilde{t}_2$  for  $\tan \beta = 15$  and  $\{m_{A^0}, \mu, A, M_{\tilde{Q}}\} = \{700, -500, 120, 300\}$  GeV as a function of the Higgsino mass parameter  $\mu$ . The electroweak corrections are almost constant

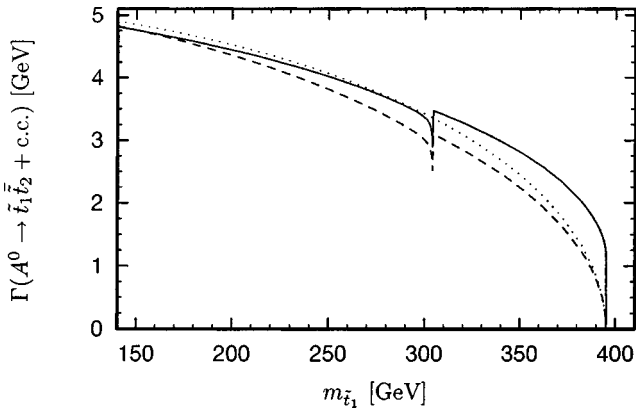


FIG. 3. Tree-level width (dotted line), full electroweak corrected decay width (dashed line) and full one-loop (electroweak and SUSY QCD) corrected width (solid line) of  $A^0 \rightarrow \tilde{t}_1 \tilde{t}_2$  as functions of  $m_{\tilde{t}_1}$ .

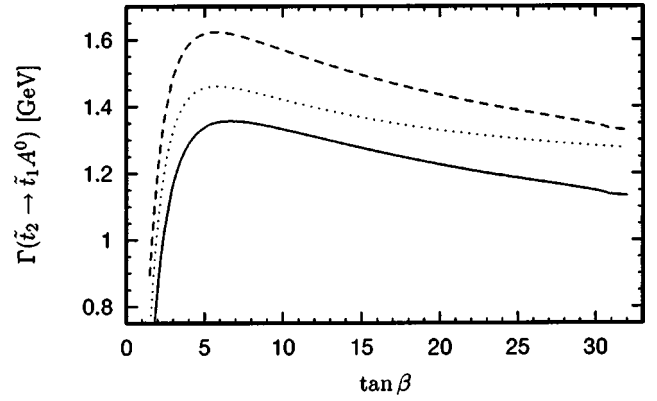


FIG. 4.  $\tan \beta$  dependence of the tree-level (dotted line), full electroweak corrected (dashed line) and full one-loop corrected (solid line) decay widths of  $\tilde{t}_2 \rightarrow \tilde{t}_1 A^0$ .

about  $-7\%$ . At  $\mu \approx -242$  GeV one can identify the pseudo-threshold coming from  $\tilde{t}_2 \rightarrow t \tilde{\chi}_4^0$ .

Figure 3 shows the tree-level, the full electroweak and the full one-loop corrected (electroweak and SUSY QCD) decay widths of  $A^0 \rightarrow \tilde{t}_1 \tilde{t}_2$  as functions of the lighter top squark mass,  $m_{\tilde{t}_1}$ , where  $M_{\tilde{Q}}$  is varied from 200 to 450 GeV. As input parameters we choose  $\{m_{A^0}, \mu, A, M_{\tilde{Q}}\} = \{900, 250, 300, 120\}$  GeV and  $\tan \beta = 7$ . Again, in a large region of the parameter space the electroweak corrections are comparable to the SUSY QCD ones. The pseudothreshold at  $m_{\tilde{t}_1} \approx 304$  GeV originates from  $\tilde{t}_2 \rightarrow t \tilde{\chi}_3^0$  in the wavefunction correction.

In Fig. 4 the dependence of the crossed channel decay width,  $\Gamma(\tilde{t}_2 \rightarrow \tilde{t}_1 A^0)$ , as a function of  $\tan \beta$  is given. We see that the electroweak corrections have different signs compared to the SUSY QCD ones and go up to 10%. As input parameters we have chosen  $\{m_{A^0}, \mu, A, M_{\tilde{Q}}\} = \{170, 500, -390, 250, 350\}$  GeV as well as  $M_{\tilde{U}_3} = 450$  GeV to get an acceptable top squark mass splitting.

Figure 5 shows the decay width  $\Gamma(\tilde{t}_2 \rightarrow \tilde{t}_1 A^0)$  as a function of  $m_{\tilde{t}_1}$ , varying  $M_{\tilde{Q}_3}$  from 200 to 460 GeV. To get a

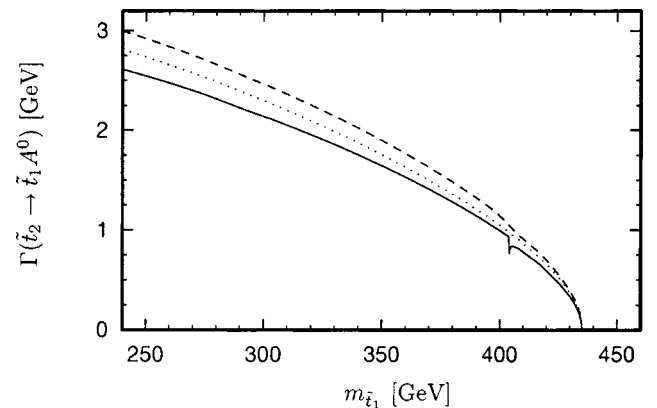


FIG. 5.  $m_{\tilde{t}_1}$  dependence of the tree-level (dotted line), full electroweak corrected (dashed line) and full one-loop corrected (solid line) decay widths of  $\tilde{t}_2 \rightarrow \tilde{t}_1 A^0$ .

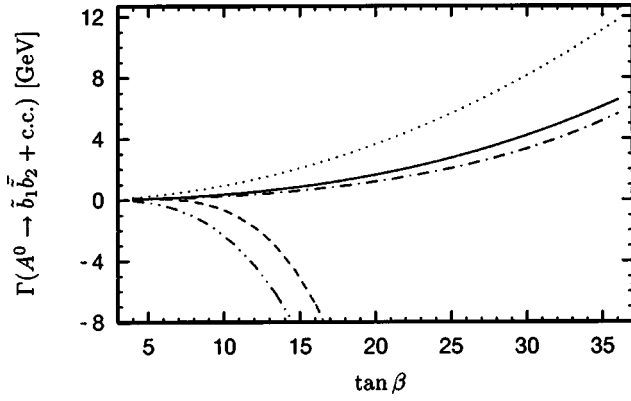


FIG. 6. Two kinds of perturbation expansion: the dotted line corresponds to the on-shell tree-level width, the dashed and dash-dot-dotted lines correspond to electroweak SUSY QCD on-shell one-loop widths, respectively. The dash-dotted line corresponds to the improved tree-level and the solid line to the (full) improved one-loop widths.

larger mass splitting for the top squarks, we relax the conditions for 3rd generation squarks and take  $\{M_{\tilde{U}_3}, M_{\tilde{D}_3}\} = \{500, 300\}$  GeV. All other SUSY breaking masses are fixed at 300 GeV. For the remaining input parameters we choose  $\{m_{A^0}, \mu, A\} = \{120, -400, -350\}$  GeV and  $\tan \beta = 7$ .

## 2. Bottom squark case

In Fig. 6 we show two kinds of perturbation expansion for  $\Gamma(A^0 \rightarrow \tilde{b}_1 \tilde{b}_2)$  with  $\{m_{A^0}, \mu, A, M, M_{\tilde{Q}}\} = \{800, -300, -500, 200, 300\}$  GeV. First we show the tree-level width, given in terms of on-shell input parameters (dotted line). The dashed and dash-dot-dotted lines correspond to the on-shell electroweak and full (electroweak plus SUSY QCD) one-loop widths, respectively. For both corrections one can clearly see the invalidity of the on-shell perturbation expansion, which leads to an improper negative decay width. The

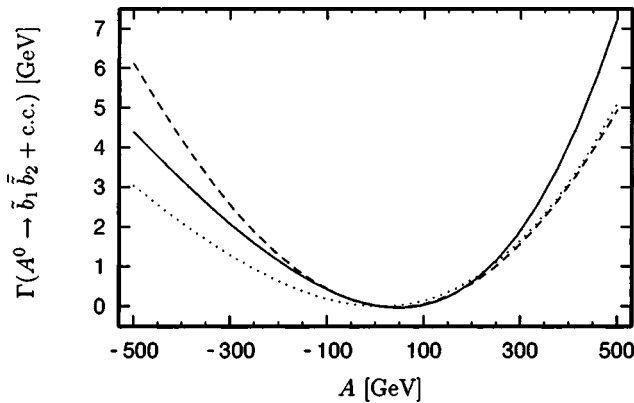


FIG. 7. Perturbation expansion around the improved tree-level decay width (dotted line) of  $\Gamma(A^0 \rightarrow \tilde{b}_1 \tilde{b}_2)$  as a function of the trilinear coupling  $A$ . Dashed and solid lines correspond to the improved SUSY QCD and full improved one-loop widths, respectively.

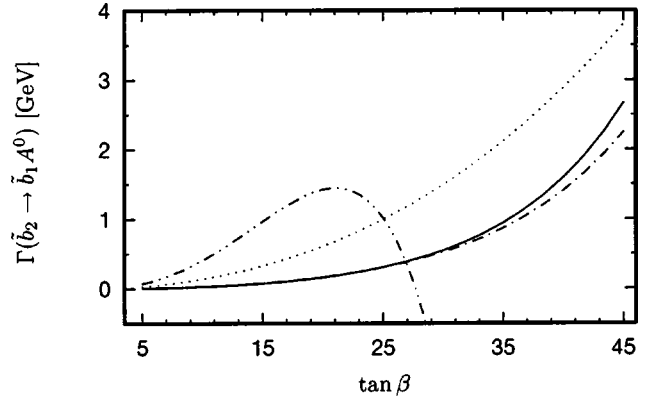


FIG. 8.  $\tan \beta$  dependence of  $\Gamma(\tilde{b}_2 \rightarrow \tilde{b}_1 A^0)$  for two kinds of perturbation expansion. The dotted and dash-dot-dotted lines correspond to on-shell tree-level and full one-loop widths, respectively, the dash-dotted line corresponds to improved tree-level width and the solid line shows the full improved one-loop width.

second method of perturbation expansion is given by the dash-dotted and the solid lines, which correspond to the improved tree-level and improved full one-loop decay widths, respectively. Here we take the same input parameters as in the first case but with running  $A = -500$  GeV.

In Fig. 7 we show the decay width  $\Gamma(A^0 \rightarrow \tilde{b}_1 \tilde{b}_2)$  as a function of  $\overline{\text{DR}}$  running  $A$  for  $\{m_{A^0}, \mu, M, M_{\tilde{Q}}\} = \{800, -300, 300, 300\}$  GeV and  $\tan \beta = 30$ . The dotted line corresponds to the improved tree-level width, the dashed line corresponds to the improved SUSY QCD one-loop width and the solid line shows the full improved one-loop width. For negative  $A$  the electroweak corrections decrease the decay width by  $\sim 20\%$ , whereas for positive  $A$  the SUSY QCD corrections almost vanish and the electroweak ones go up to 30%.

Figure 8 shows the behavior of the decay width  $\Gamma(\tilde{b}_2 \rightarrow \tilde{b}_1 A^0)$  for large  $\tan \beta$ . As in Fig. 6 two kinds of perturbation expansion are given. The dotted and dash-dot-dotted lines correspond to the tree-level and full one-loop decay

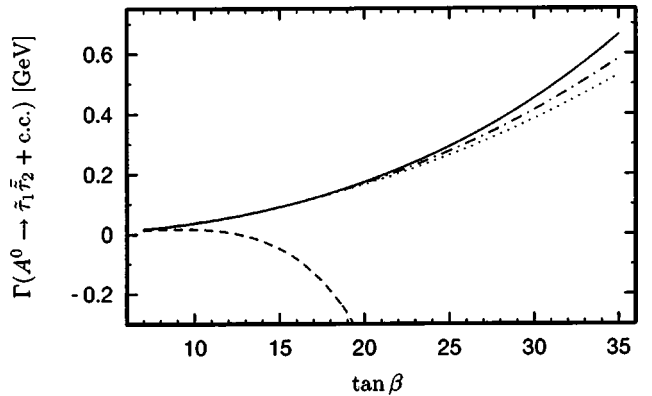


FIG. 9. On-shell tree-level (dotted line) and full electroweak on-shell corrected decay (dashed line) widths of  $A^0 \rightarrow \tilde{\tau}_1 \tilde{\tau}_2$  as a function of  $\tan \beta$ . The dash-dotted and solid lines correspond to improved tree-level and full improved one-loop decay widths.

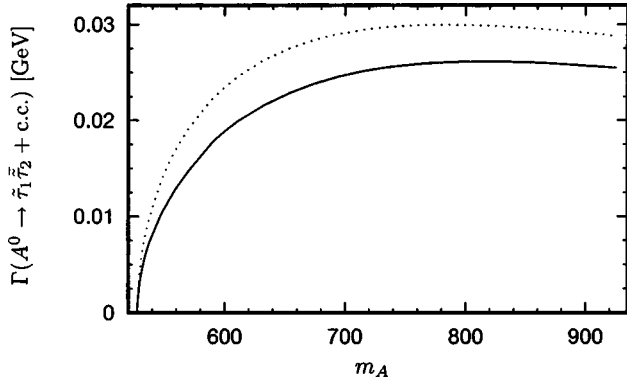


FIG. 10.  $m_{A^0}$  dependence of the improved tree-level (dotted line) and full one-loop corrected (solid line) decay widths of  $\Gamma(A^0 \rightarrow \tilde{\tau}_1 \tilde{\tau}_2)$ .

widths in the pure on-shell scheme. For large  $\tan\beta$  one can clearly see the invalidity of the perturbation series, leading to a negative decay width. In the second case we show the expansion around the tree-level decay width, given in terms of running  $A_b$  and  $m_b$ . The dash-dotted line corresponds to the improved tree-level width and the solid one to the one-loop width. Up to  $\tan\beta \sim 30$  the corrections stay relatively small, which indicates that already the (improved) tree level is a good approximation for  $\Gamma(\tilde{b}_2 \rightarrow \tilde{b}_1 A^0)$ . As input parameters we take the values  $\{m_{A^0}, \mu, A, M, M_{\tilde{Q}}\} = \{150, -220, 500, 200, 300\}$  GeV and  $M_{\tilde{D}_3} = 500$  GeV for kinematical reasons.

### 3. Stau case

In Fig. 9 the  $A^0$  decay into two staus is given as a function of  $\tan\beta$ . Despite the absence of SUSY QCD corrections the perturbation expansion around the on-shell tree-level width (dotted line) leads to an improper negative decay width (dashed line) coming from large  $\mathcal{O}(h_b^2)$  corrections. As input parameters we take  $\{m_{A^0}, \mu, A, M, M_{\tilde{Q}}\} = \{800, 400, -500, 120, 300\}$  GeV. The dash-dotted line corresponds to the improved tree-level width and the solid line shows the improved one-loop width for the same input parameters as above and running  $A = -500$  GeV.

Figure 10 shows the decay width of  $\Gamma(A^0 \rightarrow \tilde{\tau}_1 \tilde{\tau}_2)$  as a function of the mass of the decaying Higgs boson  $A^0$  for the improved perturbation expansion. The dotted and the solid lines correspond to the (improved) tree-level and full one-loop widths, respectively. In the whole region of the parameter space shown the (electroweak) corrections decrease the on-shell width by 15%. As input parameters we choose  $\{\mu, A, M, M_{\tilde{Q}}\} = \{-450, -500, 120, 260\}$  GeV and  $\tan\beta = 7$ .

In Fig. 11 we show the  $A$  dependence of  $\Gamma(\tilde{\tau}_2 \rightarrow \tilde{\tau}_1 A^0)$  in the improved case. For negative values of  $A$  the corrections increase the on-shell width by  $\sim 20\%$  whereas for positive values of  $A$  the corrections are negative and go up to 15%. The input parameters are taken as follows:  $\{m_{A^0}, \mu, M, M_{\tilde{Q}}\} = \{150, 400, 300, 300\}$  GeV and  $M_{\tilde{E}_3} = 500$  GeV for an acceptable stau mass splitting. For  $\tan\beta$  we take the value 30.

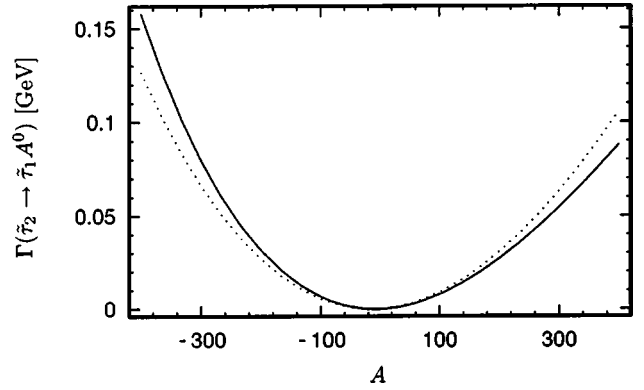


FIG. 11.  $A$  dependence of the improved tree-level (dotted line) and improved one-loop (solid line) decay widths for  $\tilde{\tau}_2 \rightarrow \tilde{\tau}_1 A^0$ .

## VI. CONCLUSIONS

We have calculated the *full* electroweak one-loop corrections to the decay widths  $A^0 \rightarrow \tilde{f}_1 \tilde{f}_2$  and  $\tilde{f}_2 \rightarrow \tilde{f}_1 A^0$  in the on-shell scheme. We have presented all formulas required for the computation. It has been necessary to renormalize almost all parameters of the MSSM. We have also included the SUSY QCD corrections which were calculated in [8]. For the decay into bottom squarks and tau sleptons for large  $\tan\beta$  an improvement of the on-shell perturbation expansion is necessary. We have worked out an iterative method to improve the one-loop calculation. Thereby, the tree-level coupling is redefined in terms of  $\overline{\text{DR}}$  running masses and running  $A_f$ . We find that the corrections are significant and in a wide range of the parameter space comparable to the SUSY QCD corrections.

## ACKNOWLEDGMENT

The authors acknowledge support from EU under the HPRN-CT-2000-00149 network program and the ‘‘Fonds zur Forderung der wissenschaftlichen Forschung’’ of Austria, Project No. P13139-PHY.

## APPENDIX A: NOTATION AND COUPLINGS

For the neutral and charged Higgs fields we use the notation  $H_k^0 = \{h^0, H^0, A^0, G^0\}$ ,  $H_k^+ = \{H^+, G^+, H^-, G^-\}$  and  $H_k^- \equiv (H_k^+)^* = \{H^-, G^-, H^+, G^+\}$ .  $t/\tilde{t}$  stands for an up-type (s)fermion and  $b/\tilde{b}$  for a down-type one. Following [2,3] the Higgs-boson-sfermion-sfermion couplings for neutral Higgs bosons,  $G_{ijk}^{\tilde{f}}$ , can be written as

$$G_{ijk}^{\tilde{f}} \equiv G(H_k^0 \tilde{f}_i \tilde{f}_j) = [R^{\tilde{f}} G_{LR,k}^{\tilde{f}} (R^{\tilde{f}})^T]_{ij}. \quad (\text{A1})$$

The 3rd generation left-right couplings  $G_{LR,k}^{\tilde{f}}$  for up- and down-type sfermions are



$$G_{LR,1}^{\tilde{t}} = \begin{pmatrix} -\sqrt{2}h_t m_t c_\alpha + g_Z m_Z (I_t^{3L} - e_t s_W^2) s_{\alpha+\beta} & -\frac{h_t}{\sqrt{2}}(A_t c_\alpha + \mu s_\alpha) \\ -\frac{h_t}{\sqrt{2}}(A_t c_\alpha + \mu s_\alpha) & -\sqrt{2}h_t m_t c_\alpha + g_Z m_Z e_t s_W^2 s_{\alpha+\beta} \end{pmatrix}, \quad (\text{A2})$$

$$G_{LR,1}^{\tilde{b}} = \begin{pmatrix} \sqrt{2}h_b m_b s_\alpha + g_Z m_Z (I_b^{3L} - e_b s_W^2) s_{\alpha+\beta} & \frac{h_b}{\sqrt{2}}(A_b s_\alpha + \mu c_\alpha) \\ \frac{h_b}{\sqrt{2}}(A_b s_\alpha + \mu c_\alpha) & \sqrt{2}h_b m_b s_\alpha + g_Z m_Z e_b s_W^2 s_{\alpha+\beta} \end{pmatrix}, \quad (\text{A3})$$

$$G_{LR,2}^{\tilde{t}} = G_{LR,1}^{\tilde{t}} \quad \text{with } \alpha \rightarrow \alpha - \pi/2, \quad (\text{A4})$$

$$G_{LR,3}^{\tilde{t}} = -\sqrt{2}h_t \begin{pmatrix} 0 & -\frac{i}{2}(A_t c_\beta + \mu s_\beta) \\ \frac{i}{2}(A_t c_\beta + \mu s_\beta) & 0 \end{pmatrix}, \quad (\text{A5})$$

$$G_{LR,3}^{\tilde{b}} = -\sqrt{2}h_b \begin{pmatrix} 0 & -\frac{i}{2}(A_b s_\beta + \mu c_\beta) \\ \frac{i}{2}(A_b s_\beta + \mu c_\beta) & 0 \end{pmatrix}, \quad (\text{A6})$$

$$G_{LR,4}^{\tilde{t}} = G_{LR,3}^{\tilde{t}} \quad \text{with } \beta \rightarrow \beta - \pi/2, \quad (\text{A7})$$

where we have used the abbreviations  $s_x \equiv \sin x$ ,  $c_x \equiv \cos x$  and  $s_W \equiv \sin \theta_W$ .  $\alpha$  denotes the mixing angle of the  $\{H^0, H^0\}$  system, and  $h_t$  and  $h_b$  are the Yukawa couplings

$$h_t = \frac{gm_t}{\sqrt{2}m_W \sin \beta}, \quad h_b = \frac{gm_b}{\sqrt{2}m_W \cos \beta}. \quad (\text{A8})$$

The couplings of charged Higgs bosons to two sfermions are given by ( $l=1,2$ )

$$G_{ijl}^{\tilde{f}\tilde{f}'} \equiv G(H_l^\pm \tilde{f}_i^* \tilde{f}_j') = G_{jil}^{\tilde{f}'\tilde{f}} = (R^{\tilde{f}} G_{LR,l}^{\tilde{f}\tilde{f}'} (R^{\tilde{f}'})^T)_{ij}, \quad (\text{A9})$$

$$G_{LR,1}^{\tilde{t}\tilde{b}} = \begin{pmatrix} h_b m_b \sin \beta + h_t m_t \cos \beta - \frac{gm_W}{\sqrt{2}} \sin 2\beta & h_b (A_b \sin \beta + \mu \cos \beta) \\ h_t (A_t \cos \beta + \mu \sin \beta) & h_t m_b \cos \beta + h_b m_t \sin \beta \end{pmatrix}, \quad (\text{A10})$$

$$G_{LR,1}^{\tilde{b}\tilde{t}} = \begin{pmatrix} h_b m_b \sin \beta + h_t m_t \cos \beta - \frac{gm_W}{\sqrt{2}} \sin 2\beta & h_t (A_t \cos \beta + \mu \sin \beta) \\ h_b (A_b \sin \beta + \mu \cos \beta) & h_t m_b \cos \beta + h_b m_t \sin \beta \end{pmatrix} = (G_{LR,1}^{\tilde{t}\tilde{b}})^T, \quad (\text{A11})$$

$$G_{LR,2}^{\tilde{f}\tilde{f}'} = G_{LR,1}^{\tilde{f}\tilde{f}'} \quad \text{with } \beta \rightarrow \beta - \frac{\pi}{2}. \quad (\text{A12})$$

$f'$  denotes the isospin partner of the fermion  $f$ , i.e.  $t' = b, \tilde{b}'_i = \tilde{t}_i$  etc. Note that only the angle  $\beta$  explicitly given in the matrices above has to be substituted; the dependence of  $\beta$  in the Yukawa couplings has to remain the same.

The  $H_k^0 H_l^0 \tilde{f}_i^* \tilde{f}_j$  interaction is given by

$$\mathcal{L} = -\frac{1}{2} \sum_f [h_f^2 c_{kl}^{\tilde{f}} \delta_{ij} + g^2 (c_{kl}^{\tilde{b}} - c_{kl}^{\tilde{t}}) e_{ij}^{\tilde{f}}] H_k^0 H_l^0 \tilde{f}_i^* \tilde{f}_j, \quad (\text{A13})$$

with

$$c_{kl}^{\tilde{b}} = \begin{pmatrix} \sin^2 \alpha & -\frac{1}{2} \sin 2\alpha & 0 & 0 \\ -\frac{1}{2} \sin 2\alpha & \cos^2 \alpha & 0 & 0 \\ 0 & 0 & \sin^2 \beta & -\frac{1}{2} \sin 2\beta \\ 0 & 0 & -\frac{1}{2} \sin 2\beta & \cos^2 \beta \end{pmatrix}, \quad (\text{A14})$$

$$c_{kl}^{\tilde{t}} = \begin{pmatrix} \cos^2 \alpha & \frac{1}{2} \sin 2\alpha & 0 & 0 \\ \frac{1}{2} \sin 2\alpha & \sin^2 \alpha & 0 & 0 \\ 0 & 0 & \cos^2 \beta & \frac{1}{2} \sin 2\beta \\ 0 & 0 & \frac{1}{2} \sin 2\beta & \sin^2 \beta \end{pmatrix}, \quad (\text{A15})$$

$$e_{ij}^{\tilde{f}} = \frac{1}{2c_W^2} [(I_f^{3L} - e_f s_W^2) R_{i1}^{\tilde{f}} R_{j1}^{\tilde{f}} + e_f s_W^2 R_{i2}^{\tilde{f}} R_{j2}^{\tilde{f}}]. \quad (\text{A16})$$

For the  $H_k^+ H_l^- \tilde{f}_i^* \tilde{f}_j$  interaction,

$$\mathcal{L} = -\frac{1}{2} \sum_f [h_f^2 d_{kl}^{\tilde{f}} (R_{i2}^{\tilde{f}} R_{j2}^{\tilde{f}} + R_{i1}^{\tilde{f}'} R_{j1}^{\tilde{f}'}) + g^2 (d_{kl}^{\tilde{b}} - d_{kl}^{\tilde{t}}) f_{ij}^{\tilde{f}}] H_k^+ H_l^- \tilde{f}_i^* \tilde{f}_j, \quad (\text{A17})$$

we use the coupling matrices

$$d_{kl}^{\tilde{b}} = \begin{pmatrix} \sin^2 \beta & -\frac{1}{2} \sin 2\beta & 0 & 0 \\ -\frac{1}{2} \sin 2\beta & \cos^2 \beta & 0 & 0 \\ 0 & 0 & \sin^2 \beta & -\frac{1}{2} \sin 2\beta \\ 0 & 0 & -\frac{1}{2} \sin 2\beta & \cos^2 \beta \end{pmatrix}, \quad (\text{A18})$$

$$d_{kl}^{\tilde{t}} = \begin{pmatrix} \cos^2 \beta & \frac{1}{2} \sin 2\beta & 0 & 0 \\ \frac{1}{2} \sin 2\beta & \sin^2 \beta & 0 & 0 \\ 0 & 0 & \cos^2 \beta & \frac{1}{2} \sin 2\beta \\ 0 & 0 & \frac{1}{2} \sin 2\beta & \sin^2 \beta \end{pmatrix}, \quad (\text{A19})$$

$$f_{ij}^{\tilde{f}} = \frac{1}{2c_W^2} [(-I_f^{3L} \cos 2\theta_W - e_f s_W^2) R_{i1}^{\tilde{f}} R_{j1}^{\tilde{f}} + e_f s_W^2 R_{i2}^{\tilde{f}} R_{j2}^{\tilde{f}}]. \quad (\text{A20})$$

For the Higgs-boson-fermion-fermion couplings the interaction Lagrangian reads

$$\begin{aligned} \mathcal{L} = & \sum_{k=1}^2 s_k^f H_k^0 \bar{f} f + \sum_{k=3}^4 s_k^f H_k^0 \bar{f} \gamma^5 f \\ & + \sum_{l=1}^2 [H_l^+ \bar{l} (y_l^b P_R + y_l^t P_L) b + \text{H.c.}] \quad (\text{A21}) \end{aligned}$$

with the couplings

$$s_1^t = -g \frac{m_t \cos \alpha}{2m_W \sin \beta} = -\frac{h_t}{\sqrt{2}} \cos \alpha,$$

$$s_1^b = g \frac{m_b \sin \alpha}{2m_W \cos \beta} = \frac{h_b}{\sqrt{2}} \sin \alpha,$$

$$s_2^t = -g \frac{m_t \sin \alpha}{2m_W \sin \beta} = -\frac{h_t}{\sqrt{2}} \sin \alpha,$$

$$s_2^b = -g \frac{m_b \cos \alpha}{2m_W \cos \beta} = -\frac{h_b}{\sqrt{2}} \cos \alpha,$$

$$s_3^t = i g \frac{m_t \cot \beta}{2m_W} = i \frac{h_t}{\sqrt{2}} \cos \beta,$$

$$s_3^b = i g \frac{m_b \tan \beta}{2m_W} = i \frac{h_b}{\sqrt{2}} \sin \beta,$$

$$s_4^t = i g \frac{m_t}{2m_W} = i \frac{h_t}{\sqrt{2}} \sin \beta,$$

$$s_4^b = -i g \frac{m_b}{2m_W} = -i \frac{h_b}{\sqrt{2}} \cos \beta,$$

$$y_1^t = g \frac{m_t \cot \beta}{\sqrt{2}m_W} = h_t \cos \beta,$$

$$y_1^b = g \frac{m_b \tan \beta}{\sqrt{2}m_W} = h_b \sin \beta,$$

$$y_2^t = g \frac{m_t}{\sqrt{2}m_W} = h_t \sin \beta, \quad y_2^b = -g \frac{m_b}{\sqrt{2}m_W} = -h_b \cos \beta. \quad (\text{A22})$$

The interaction Lagrangian for Higgs bosons and gauginos is given by

$$\begin{aligned} \mathcal{L} = & -\frac{g}{2} \sum_{k=1}^2 H_k^0 \tilde{\chi}_l^0 F_{lmk}^0 \tilde{\chi}_m^0 - i \frac{g}{2} \sum_{k=3}^4 H_k^0 \tilde{\chi}_l^0 F_{lmk}^0 \gamma_5 \tilde{\chi}_m^0 \\ & - g \sum_{k=1}^2 H_k^0 \tilde{\chi}_i^+ (F_{ijk}^+ P_R + F_{jik}^+ P_L) \tilde{\chi}_j^+ \\ & + i g \sum_{k=3}^4 H_k^0 \tilde{\chi}_i^+ (F_{ijk}^+ P_R + F_{jik}^+ P_L) \tilde{\chi}_j^+ \\ & - g \sum_{k=1}^2 [H_k^+ \tilde{\chi}_i^+ (F_{ilk}^R P_R + F_{ilk}^L P_L) \tilde{\chi}_l^0 + \text{H.c.}] \quad (\text{A23}) \end{aligned}$$

with

$$\begin{aligned} F_{lmk}^0 = & \frac{e_k}{2} [Z_{l3} Z_{m2} + Z_{m3} Z_{l2} - \tan \theta_W (Z_{l3} Z_{m1} + Z_{m3} Z_{l1})] \\ & + \frac{d_k}{2} [Z_{l4} Z_{m2} + Z_{m4} Z_{l2} - \tan \theta_W (Z_{l4} Z_{m1} + Z_{m4} Z_{l1})] \\ = & F_{mlk}^0, \quad (\text{A24}) \end{aligned}$$

$$F_{ijk}^+ = \frac{1}{\sqrt{2}} (e_k V_{i1} U_{j2} - d_k V_{i2} U_{j1}), \quad (\text{A25})$$

and

$$\begin{aligned} F_{ilk}^R = & d_{k+2} \left[ V_{i1} Z_{l4} + \frac{1}{\sqrt{2}} (Z_{l2} + Z_{l1} \tan \theta_W) V_{i2} \right], \\ F_{ilk}^L = & -e_{k+2} \left[ U_{i1} Z_{l3} - \frac{1}{\sqrt{2}} (Z_{l2} + Z_{l1} \tan \theta_W) U_{i2} \right]. \quad (\text{A26}) \end{aligned}$$

$U, V$  and  $Z$  are rotation matrices that diagonalize the chargino and neutralino mass matrices.  $d_k$  and  $e_k$  take the values

$$\begin{aligned} d_k = & \{-\cos \alpha, -\sin \alpha, \cos \beta, \sin \beta\}, \\ e_k = & \{-\sin \alpha, \cos \alpha, -\sin \beta, \cos \beta\}. \quad (\text{A27}) \end{aligned}$$

The coupling of the vector boson  $Z^0$  to two sfermions,  $\mathcal{L} = -i g_Z z_{ij}^f Z_\mu^0 \tilde{f}_i^* \partial^\mu \tilde{f}_j$  with  $g_Z = g/\cos \theta_W$ , is given by the matrix

$$z_{ij}^f = C_L^f R_{i1}^{\tilde{f}} R_{j1}^{\tilde{f}} + C_R^f R_{i2}^{\tilde{f}} R_{j2}^{\tilde{f}} \quad (\text{A28})$$

with  $C_L^f = I_f^{3L} - e_f s_W^2$  and  $C_R^f = -e_f s_W^2$ .

For the interaction of a vector boson with two gauginos we use the couplings

$$O_{ij}^L = Z_{i2}V_{j1} - \frac{1}{\sqrt{2}}Z_{i4}V_{j2}, \quad O_{ij}^R = Z_{i2}U_{j1} + \frac{1}{\sqrt{2}}Z_{i3}U_{j2}, \quad (\text{A29})$$

$$O'_{ij}{}^L = -V_{i1}V_{j1} - \frac{1}{2}V_{i2}V_{j2} + \delta_{ij}s_W^2, \quad (\text{A30})$$

$$O'_{ij}{}^R = -U_{i1}U_{j1} - \frac{1}{2}U_{i2}U_{j2} + \delta_{ij}s_W^2, \quad (\text{A31})$$

$$O''_{ij}{}^L = -\frac{1}{2}Z_{i3}Z_{j3} + \frac{1}{2}Z_{i4}Z_{j4} = -O''_{ij}{}^R. \quad (\text{A32})$$

The interaction Lagrangian of the chargino-sfermion-fermion couplings is given by

$$\begin{aligned} \mathcal{L} = & \bar{l}(l_{ij}^{\tilde{b}}P_R + k_{ij}^{\tilde{b}}P_L)\tilde{\chi}_j^+ \bar{b}_i + \bar{b}(l_{ij}^{\tilde{t}}P_R + k_{ij}^{\tilde{t}}P_L)\tilde{\chi}_j^{+c} \bar{t}_i \\ & + \bar{\chi}_j^+(l_{ij}^{\tilde{b}}P_L + k_{ij}^{\tilde{b}}P_R)t\tilde{b}_i^* + \bar{\chi}_j^{+c}(l_{ij}^{\tilde{t}}P_L + k_{ij}^{\tilde{t}}P_R)b\tilde{t}_i^* \end{aligned} \quad (\text{A33})$$

with the coupling matrices

$$\begin{aligned} l_{ij}^{\tilde{t}} &= -gV_{j1}R_{i1}^{\tilde{t}} + h_tV_{j2}R_{i2}^{\tilde{t}}, & l_{ij}^{\tilde{b}} &= -gU_{j1}R_{i1}^{\tilde{b}} + h_bU_{j2}R_{i2}^{\tilde{b}}, \\ k_{ij}^{\tilde{t}} &= h_bU_{j2}R_{i1}^{\tilde{t}}, & k_{ij}^{\tilde{b}} &= h_tV_{j2}R_{i1}^{\tilde{b}}. \end{aligned} \quad (\text{A34})$$

For the neutralino-sfermion-fermion couplings the Lagrangian reads

$$\mathcal{L} = \bar{f}(a_{ik}^{\tilde{f}}P_R + b_{ik}^{\tilde{f}}P_L)\tilde{\chi}_k^0 \bar{f}_i + \bar{\chi}_k^0(a_{ik}^{\tilde{f}}P_L + b_{ik}^{\tilde{f}}P_R)f\tilde{f}_i^* \quad (\text{A35})$$

with the coupling matrices

$$a_{ik}^{\tilde{f}} = h_f Z_{kx} R_{i2}^{\tilde{f}} + g f_{Lk}^f R_{i1}^{\tilde{f}}, \quad b_{ik}^{\tilde{f}} = h_f Z_{kx} R_{i1}^{\tilde{f}} + g f_{Rk}^f R_{i2}^{\tilde{f}} \quad (\text{A36})$$

and

$$\begin{aligned} f_{Lk}^f &= \sqrt{2}[(e_f - I_f^{3L})\tan\theta_W Z_{k1} + I_f^{3L} Z_{k2}], \\ f_{Rk}^f &= -\sqrt{2}e_f \tan\theta_W Z_{k1}. \end{aligned} \quad (\text{A37})$$

$x$  takes the values {3,4} for {down, up}-type cases, respectively.

$$\begin{aligned} \delta G_{123}^{\tilde{f}(v,\tilde{f}HH)} &= -\frac{1}{(4\pi)^2} \frac{g_Z m_Z}{2} \sum_{m=1}^2 \left( \sum_{k=1}^2 \sum_{l=3}^4 G_{imk}^{\tilde{f}} G_{mjl}^{\tilde{f}} A_{k,l-2} + \sum_{k=3}^4 \sum_{l=1}^2 G_{imk}^{\tilde{f}} G_{mjl}^{\tilde{f}} A_{l,k-2} \right) C_0(m_{\tilde{f}_i}^2, m_{A^0}^2, m_{\tilde{f}_j}^2, m_{\tilde{f}_m}^2, m_{H_k^0}^2, m_{H_l^0}^2) \\ &\quad - \frac{i}{(4\pi)^2} I_f^{3L} g m_W \sum_{m=1}^2 [G_{im1}^{\tilde{f}\tilde{f}'} G_{jm2}^{\tilde{f}\tilde{f}'} C_0(m_{\tilde{f}_i}^2, m_{A^0}^2, m_{\tilde{f}_j}^2, m_{\tilde{f}_m}^2, m_{H^+}^2, m_{G^+}^2) \\ &\quad - G_{im2}^{\tilde{f}\tilde{f}'} G_{jm1}^{\tilde{f}\tilde{f}'} C_0(m_{\tilde{f}_i}^2, m_{A^0}^2, m_{\tilde{f}_j}^2, m_{\tilde{f}_m}^2, m_{G^+}^2, m_{H^+}^2)] \end{aligned} \quad (\text{B4})$$

with

## APPENDIX B: VERTEX CORRECTIONS

Here we give the explicit form of the electroweak contributions to the vertex corrections which are depicted in Fig. 12. For SUSY QCD contributions we refer to [8].

$$\begin{aligned} \delta G_{123}^{\tilde{f}(v)} &= \delta G_{123}^{\tilde{f}(v,H\tilde{f}\tilde{f})} + \delta G_{123}^{\tilde{f}(v,\tilde{f}HH)} + \delta G_{123}^{\tilde{f}(v,\tilde{\chi}ff)} + \delta G_{123}^{\tilde{f}(v,\tilde{f}\tilde{\chi}\tilde{\chi})} \\ &\quad + \delta G_{123}^{\tilde{f}(v,V)} + \delta G_{123}^{\tilde{f}(v,\tilde{f}\tilde{f})} + \delta G_{123}^{\tilde{f}(v,H\tilde{f})} + \delta G_{123}^{\tilde{f}(v,AZ)} \\ &\quad + \delta G_{123}^{\tilde{f}(v,AG)}. \end{aligned} \quad (\text{B1})$$

The single contributions correspond to the diagrams with three scalar particles ( $\delta G_{123}^{\tilde{f}(v,H\tilde{f}\tilde{f})}$  and  $\delta G_{123}^{\tilde{f}(v,HH\tilde{f})}$ ), three fermions ( $\delta G_{123}^{\tilde{f}(v,\tilde{\chi}ff)}$  and  $\delta G_{123}^{\tilde{f}(v,\tilde{f}\tilde{\chi}\tilde{\chi})}$ ), one vector particle ( $\delta G_{123}^{\tilde{f}(v,V)}$ ) or two scalar particles ( $\delta G_{123}^{\tilde{f}(v,\tilde{f}\tilde{f})}$  and  $\delta G_{123}^{\tilde{f}(v,H\tilde{f})}$ ) in the loop.  $\delta G_{123}^{\tilde{f}(v,AZ^{\text{mix}})}$  denotes the correction due to the mixing of  $A^0$  and  $Z^0$  and  $\delta G_{123}^{\tilde{f}(v,AG)}$  is the Higgs boson mixing transition  $A^0$ - $G^0$ .

As shown in [12] we can sum up the  $A^0 Z^0$  and  $A^0 G^0$  transition amplitudes which leads to

$$\delta G_{123}^{\tilde{f}(v,AZ)} + \delta G_{123}^{\tilde{f}(v,AG)} = -\frac{i}{m_Z} \Pi_{AZ}(m_{A^0}^2) G_{124}^{\tilde{f}}. \quad (\text{B2})$$

The explicit form of the  $A^0$ - $Z^0$  self-energy,  $\Pi_{AZ}(m_{A^0}^2)$ , is given in Appendix D 1. The vertex corrections from the exchange of one Higgs boson and two sfermions are

$$\begin{aligned} \delta G_{123}^{\tilde{f}(v,H\tilde{f}\tilde{f})} &= -\frac{1}{(4\pi)^2} \sum_{m,n=1}^2 \sum_{k=1}^4 G_{mn3}^{\tilde{f}} G_{imk}^{\tilde{f}} G_{njk}^{\tilde{f}} \\ &\quad \times C_0(m_{\tilde{f}_i}^2, m_{A^0}^2, m_{\tilde{f}_j}^2, m_{H_k^0}^2, m_{\tilde{f}_m}^2, m_{\tilde{f}_n}^2) \\ &\quad - \frac{1}{(4\pi)^2} \sum_{m,n=1}^2 \sum_{k=1}^2 G_{mn3}^{\tilde{f}'} G_{imk}^{\tilde{f}\tilde{f}'} G_{jnk}^{\tilde{f}\tilde{f}'} \\ &\quad \times C_0(m_{\tilde{f}_i}^2, m_{A^0}^2, m_{\tilde{f}_j}^2, m_{H_k^+}^2, m_{\tilde{f}_m}^2, m_{\tilde{f}_n}^2) \end{aligned} \quad (\text{B3})$$

with the standard two-point function  $C_0$  [23] for which we follow the conventions of [24]. The graph with 2 Higgs particles and one sfermion in the loop leads to

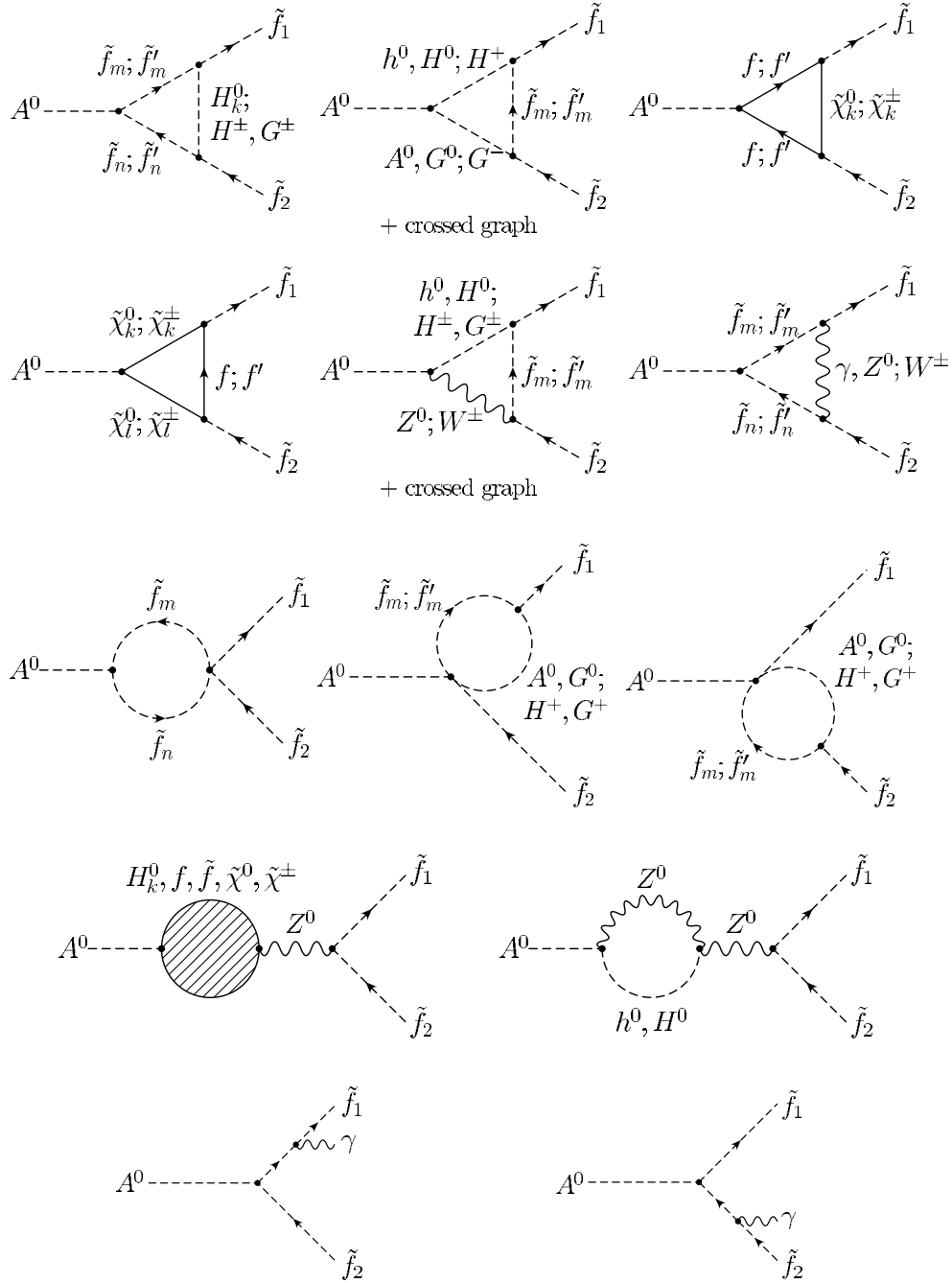


FIG. 12. Vertex and photon emission diagrams relevant to the calculation of the virtual electroweak corrections to the decay width  $A^0 \rightarrow \tilde{f}_1 \tilde{f}_2$ .

$$A_{kl} = \begin{pmatrix} -\cos 2\beta \sin(\alpha + \beta) & -\sin 2\beta \sin(\alpha + \beta) \\ \cos 2\beta \cos(\alpha + \beta) & \sin 2\beta \cos(\alpha + \beta) \end{pmatrix}. \quad (\text{B5})$$

For the gaugino exchange contributions we get

$$\begin{aligned} \delta G_{123}^{\tilde{f}(v, \tilde{\chi}ff)} &= \frac{1}{(4\pi)^2} \sum_{k=1}^4 F(m_{\tilde{f}_i}^2, m_{A^0}^2, m_{\tilde{f}_j}^2, m_{\tilde{\chi}_k^0}, m_f, m_f; s_3^f, -s_3^f, b_{ik}^{\tilde{f}}, a_{ik}^{\tilde{f}}, a_{jk}^{\tilde{f}}, b_{jk}^{\tilde{f}}) \\ &+ \frac{1}{(4\pi)^2} \sum_{k=1}^2 F(m_{\tilde{f}_i}^2, m_{A^0}^2, m_{\tilde{f}_j}^2, m_{\tilde{\chi}_k^+}, m_{f'}, m_{f'}; s_3^{f'}, -s_3^{f'}, k_{ik}^{\tilde{f}}, l_{ik}^{\tilde{f}}, l_{jk}^{\tilde{f}}, k_{jk}^{\tilde{f}}), \end{aligned} \quad (\text{B6})$$



$$\begin{aligned} \delta G_{123}^{\tilde{f}(v, f \tilde{\chi} \tilde{\chi})} &= \frac{1}{(4\pi)^2} \sum_{k,l=1}^4 F(m_{\tilde{f}_i}^2, m_{A^0}^2, m_{\tilde{f}_j}^2, m_f, m_{\tilde{\chi}_k^0}, m_{\tilde{\chi}_l^0}; i g F_{lk3}^0, -i g F_{lk3}^0, b_{ik}^{\tilde{f}}, a_{ik}^{\tilde{f}}, a_{jl}^{\tilde{f}}, b_{jl}^{\tilde{f}}) \\ &+ \frac{1}{(4\pi)^2} \sum_{k,l=1}^2 F(m_{\tilde{f}_i}^2, m_{A^0}^2, m_{\tilde{f}_j}^2, m_{f'}, m_{\tilde{\chi}_k^+}, m_{\tilde{\chi}_l^+}; i g \tilde{F}_{kl3}^+, -i g \tilde{F}_{kl3}^+, k_{ik}^{\tilde{f}}, l_{ik}^{\tilde{f}}, l_{jl}^{\tilde{f}}, k_{jl}^{\tilde{f}}), \end{aligned} \quad (\text{B7})$$

where  $F(\dots)$  is shorthand for

$$\begin{aligned} F(m_1^2, m_0^2, m_2^2, M_0, M_1, M_2; g_0^R, g_0^L, g_1^R, g_1^L, g_2^R, g_2^L) &= (h_1 M_1 + h_2 M_2) B_0(m_0^2, M_1^2, M_2^2) + (h_0 M_0 + h_1 M_1) B_0(m_1^2, M_0^2, M_1^2) \\ &+ (h_0 M_0 + h_2 M_2) B_0(m_2^2, M_0^2, M_2^2) + [2(g_0^R g_1^R g_2^R + g_0^L g_1^L g_2^L) M_0 M_1 M_2 \\ &+ h_0 M_0 (M_1^2 + M_2^2 - m_0^2) + h_1 M_1 (M_0^2 + M_2^2 - m_2^2) \\ &+ h_2 M_2 (M_0^2 + M_1^2 - m_1^2)] C_0(m_1^2, m_0^2, m_2^2, M_0^2, M_1^2, M_2^2) \end{aligned} \quad (\text{B8})$$

with the abbreviations  $h_0 = (g_0^L g_1^R g_2^R + g_0^R g_1^L g_2^L)$ ,  $h_1 = (g_0^L g_1^L g_2^R + g_0^R g_1^R g_2^L)$  and  $h_2 = (g_0^R g_1^L g_2^R + g_0^L g_1^R g_2^L)$ . For up-type sfermions  $\tilde{F}_{kl3}^+ = F_{kl3}^+$  and for down-type sfermions chargino indices are interchanged,  $\tilde{F}_{kl3}^+ = F_{lk3}^+$ . We split the irreducible vertex graphs with one vector particle in the loop into the single contributions of the photon, the  $Z$  boson and the  $W$  boson,

$$\delta G_{123}^{\tilde{f}(v, V)} = \delta G_{123}^{\tilde{f}(v, \gamma)} + \delta G_{123}^{\tilde{f}(v, Z)} + \delta G_{123}^{\tilde{f}(v, W)}. \quad (\text{B9})$$

In order to regularize the infrared divergences we introduce a photon mass  $\lambda$ . Thus we have

$$\delta G_{123}^{\tilde{f}(v, \gamma)} = \frac{1}{(4\pi)^2} (e_0 e_f)^2 G_{123}^{\tilde{f}} V(m_{\tilde{f}_i}^2, m_{A^0}^2, m_{\tilde{f}_j}^2, \lambda^2, m_{\tilde{f}_i}^2, m_{\tilde{f}_j}^2), \quad (\text{B10})$$

$$\begin{aligned} \delta G_{123}^{\tilde{f}(v, Z)} &= \frac{1}{(4\pi)^2} g_Z^2 \sum_{m,n=1}^2 G_{mn3}^{\tilde{f}} z_{im}^{\tilde{f}} z_{nj}^{\tilde{f}} V(m_{\tilde{f}_i}^2, m_{A^0}^2, m_{\tilde{f}_j}^2, m_Z^2, m_{\tilde{f}_m}^2, m_{\tilde{f}_n}^2) \\ &- \frac{i}{(4\pi)^2} \frac{g_Z^2}{2} \sum_{k,m=1}^2 G_{mjk}^{\tilde{f}} z_{im}^{\tilde{f}} R_{1k}(\alpha - \beta) V(m_{A^0}^2, m_{\tilde{f}_j}^2, m_{\tilde{f}_i}^2, m_Z^2, m_{H_k^0}^2, m_{\tilde{f}_m}^2) \\ &+ \frac{i}{(4\pi)^2} \frac{g_Z^2}{2} \sum_{k,m=1}^2 G_{imk}^{\tilde{f}} z_{mj}^{\tilde{f}} R_{1k}(\alpha - \beta) V(m_{\tilde{f}_j}^2, m_{\tilde{f}_i}^2, m_{A^0}^2, m_Z^2, m_{\tilde{f}_m}^2, m_{H_k^0}^2), \end{aligned} \quad (\text{B11})$$

$$\begin{aligned} \delta G_{123}^{\tilde{f}(v, W)} &= \frac{1}{(4\pi)^2} \frac{g^2}{2} \sum_{m,n=1}^2 G_{mn3}^{\tilde{f}'} R_{i1}^{\tilde{f}} R_{j1}^{\tilde{f}'} R_{m1}^{\tilde{f}'} R_{n1}^{\tilde{f}'} V(m_{\tilde{f}_i}^2, m_{A^0}^2, m_{\tilde{f}_j}^2, m_W^2, m_{\tilde{f}_m}^2, m_{\tilde{f}_n}^2) \\ &+ \frac{i}{(4\pi)^2} \frac{g^2}{2\sqrt{2}} \sum_{m=1}^2 G_{jm1}^{\tilde{f}'} R_{i1}^{\tilde{f}} R_{m1}^{\tilde{f}'} V(m_{A^0}^2, m_{\tilde{f}_j}^2, m_{\tilde{f}_i}^2, m_W^2, m_{H^+}^2, m_{\tilde{f}_m}^2) \\ &- \frac{i}{(4\pi)^2} \frac{g^2}{2\sqrt{2}} \sum_{m=1}^2 G_{im1}^{\tilde{f}'} R_{m1}^{\tilde{f}'} R_{j1}^{\tilde{f}} V(m_{\tilde{f}_j}^2, m_{\tilde{f}_i}^2, m_{A^0}^2, m_W^2, m_{\tilde{f}_m}^2, m_{H^+}^2), \end{aligned} \quad (\text{B12})$$

where we have used the vector vertex function

$$\begin{aligned} V(m_1^2, m_0^2, m_2^2, M_0^2, M_1^2, M_2^2) &= -B_0(m_0^2, M_1^2, M_2^2) + B_0(m_1^2, M_0^2, M_1^2) + B_0(m_2^2, M_0^2, M_2^2) \\ &+ (-2m_0^2 + m_1^2 + m_2^2 - M_0^2 + M_1^2 + M_2^2) C_0(m_1^2, m_0^2, m_2^2, M_0^2, M_1^2, M_2^2) \end{aligned} \quad (\text{B13})$$

and the rotation matrix  $R_{kl}$ ,

$$R_{kl}(\phi) \equiv \begin{pmatrix} \cos \phi & \sin \phi \\ -\sin \phi & \cos \phi \end{pmatrix}_{kl}. \quad (\text{B14})$$

For the vertex graphs with 2 sfermions in the loop we obtain

$$\begin{aligned}
\delta G_{123}^{\tilde{f}(v,\tilde{f}\tilde{f})} = & -\frac{1}{(4\pi)^2} h_f^2 \sum_{m,n=1}^2 G_{nm3}^{\tilde{f}} [R_{ijmn}^{\tilde{f}} + R_{mni j}^{\tilde{f}} + N_C^f (R_{inmj}^{\tilde{f}} + R_{mj in}^{\tilde{f}})] B_0(m_{A^0}^2, m_{\tilde{f}_m}^2, m_{\tilde{f}_n}^2) \\
& -\frac{1}{(4\pi)^2} g_Z^2 \sum_{m,n=1}^2 G_{nm3}^{\tilde{f}} \left[ \left( \frac{1}{4} - (2I_f^{3L} - e_f) e_f s_W^2 \right) R_{ijmn}^{\tilde{f}L} + e_f^2 s_W^2 R_{ijmn}^{\tilde{f}R} \right] (N_C^f + 1) + (I_f^{3L} - e_f) e_f s_W^2 [N_C^f (R_{ijmn}^{\tilde{f}} + R_{mni j}^{\tilde{f}}) \\
& + R_{inmj}^{\tilde{f}} + R_{mj in}^{\tilde{f}}] \left. \right\} B_0(m_{A^0}^2, m_{\tilde{f}_m}^2, m_{\tilde{f}_n}^2) - \frac{1}{(4\pi)^2} N_C^{\hat{f}} h_f h_{\hat{f}} \sum_{m,n=1}^2 G_{nm3}^{\hat{f}} (R_{ijnm}^{\hat{f}\tilde{f}\tilde{f}} + R_{jimn}^{\hat{f}\tilde{f}\tilde{f}}) B_0(m_{A^0}^2, m_{\tilde{f}_m}^2, m_{\tilde{f}_n}^2). \quad (B15)
\end{aligned}$$

For various products of sfermion rotation matrices we have introduced the short forms

$$\begin{aligned}
R_{ijkl}^{\tilde{f}L} &= R_{i1}^{\tilde{f}} R_{j1}^{\tilde{f}} R_{k1}^{\tilde{f}} R_{l1}^{\tilde{f}}, & R_{ijkl}^{\tilde{f}} &= R_{i1}^{\tilde{f}} R_{j1}^{\tilde{f}} R_{k2}^{\tilde{f}} R_{l2}^{\tilde{f}}, \\
R_{ijkl}^{\tilde{f}R} &= R_{i2}^{\tilde{f}} R_{j2}^{\tilde{f}} R_{k2}^{\tilde{f}} R_{l2}^{\tilde{f}}, & R_{ijkl}^{\hat{f}\tilde{f}\tilde{f}} &= R_{i1}^{\tilde{f}} R_{j2}^{\tilde{f}} R_{k1}^{\hat{f}} R_{l2}^{\hat{f}}. \quad (B16)
\end{aligned}$$

Note that the last term in Eq. (B15) originates from the mixing of 2 squarks and 2 sleptons, where  $\hat{f}$  denotes the ‘‘family partner’’ of the fermion  $f$  with the same isospin and from the same generation, i.e.  $\hat{i} = \nu_\tau$  or  $\hat{\tau}_i = \tilde{b}_i$ . The diagrams with one Higgs boson and one sfermion in the loop lead to

$$\begin{aligned}
\delta G_{123}^{\tilde{f}(v,H\tilde{f})} = & -\frac{1}{(4\pi)^2} \sum_{k=3}^4 \sum_{m=1}^2 G_{imk}^{\tilde{f}} [h_f^2 c_{3k}^{\tilde{f}} \delta_{mj} + g^2 (c_{3k}^{\tilde{b}} - c_{3k}^{\tilde{t}}) e_{mj}^{\tilde{f}}] B_0(m_{A^0}^2, m_{H_k^0}^2, m_{\tilde{f}_m}^2) \\
& + \frac{i}{(4\pi)^2} \sqrt{2} I_f^{3L} \sum_{k,m=1}^2 G_{imk}^{\tilde{f}\tilde{f}'} \left[ \begin{aligned} & \left\{ (h_\uparrow^2 - g^2/2) \cos^2 \beta - (h_\downarrow^2 - g^2/2) \sin^2 \beta \right\} R_{m1}^{\tilde{f}'} R_{j1}^{\tilde{f}} \\ & \left\{ (h_f^2 + h_{f'}^2 - g^2) \sin \beta \cos \beta \right\} \end{aligned} \right] \\
& + h_f h_{f'} \delta_{k2} R_{m2}^{\tilde{f}'} R_{j2}^{\tilde{f}} \left. \right] B_0(m_{A^0}^2, m_{H_k^+}^2, m_{\tilde{f}_m}^2) - i \leftrightarrow j. \quad (B17)
\end{aligned}$$

with  $h_\uparrow = \{h_t, 0\}$  and  $h_\downarrow = \{h_b, h_\tau\}$  for the decay into {squarks, sleptons}, respectively. The Higgs-boson-sfermion coupling matrices  $c_{kl}^{\tilde{f}}$  and  $e_{ij}^{\tilde{f}}$  can be found in Appendix A.

### APPENDIX C: DIAGONAL WAVE-FUNCTION CORRECTIONS

For the diagonal wave-function renormalization constants we use the conventional on-shell renormalization conditions which lead to

$$\delta Z_{33}^H = -\mathfrak{A} \dot{\Pi}_{33}^H(m_{A^0}^2), \quad \delta Z_{ii}^{\tilde{f}} = -\mathfrak{A} \dot{\Pi}_{ii}^{\tilde{f}}(m_{\tilde{f}_i}^2), \quad (C1)$$

where the overdot in  $\dot{\Pi}_{ii}(k^2)$  denotes the derivative with respect to  $k^2$ . In the following we list the single contributions of the wave-function corrections (Figs. 13 and 14).

#### 1. Higgs boson part

$$\begin{aligned}
\delta Z_{33}^{H,f} = & \frac{2}{(4\pi)^2} \sum_f N_C^f (s_f^2)^2 [B_0(m_{A^0}^2, m_f^2, m_f^2) \\
& + m_{A^0}^2 \dot{B}_0(m_{A^0}^2, m_f^2, m_f^2)], \quad (C2)
\end{aligned}$$

$$\begin{aligned}
\delta Z_{33}^{H,\tilde{f}} = & -\frac{1}{(4\pi)^2} \sum_f \sum_{m,n=1}^2 N_C^f G_{mn3}^{\tilde{f}} G_{nm3}^{\tilde{f}} \\
& \times \dot{B}_0(m_{A^0}^2, m_{\tilde{f}_m}^2, m_{\tilde{f}_n}^2), \quad (C3)
\end{aligned}$$

$$\begin{aligned}
\delta Z_{33}^{H,\tilde{\chi}^0} = & \frac{1}{(4\pi)^2} g^2 \sum_{k,l=1}^4 (F_{kl3}^0)^2 [\dot{B}_0(m_{A^0}^2, m_{\tilde{\chi}_k^0}^2, m_{\tilde{\chi}_l^0}^2) \\
& \times [(m_{\tilde{\chi}_k^0}^2 - m_{\tilde{\chi}_l^0}^2)^2 - m_{A^0}^2] - B_0(m_{A^0}^2, m_{\tilde{\chi}_k^0}^2, m_{\tilde{\chi}_l^0}^2)], \quad (C4)
\end{aligned}$$

$$\begin{aligned}
\delta Z_{33}^{H,\tilde{\chi}^+} = & \frac{1}{(4\pi)^2} g^2 \sum_{k,l=1}^2 \{((F_{kl3}^+)^2 + (F_{lk3}^+)^2) \\
& \times [(m_{\tilde{\chi}_k^+}^2 + m_{\tilde{\chi}_l^+}^2 - m_{A^0}^2) \dot{B}_0 - B_0] \\
& - 4m_{\tilde{\chi}_k^+} m_{\tilde{\chi}_l^+} F_{kl3}^+ F_{lk3}^+ \dot{B}_0\} (m_{A^0}^2, m_{\tilde{\chi}_k^+}^2, m_{\tilde{\chi}_l^+}^2), \quad (C5)
\end{aligned}$$

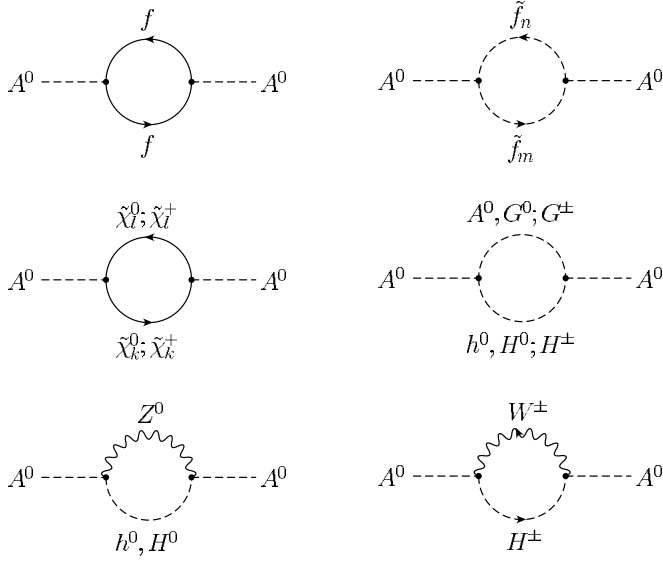


FIG. 13. Diagonal Higgs boson self-energies.

$$\begin{aligned} \delta Z_{33}^{H,H} = & -\frac{1}{(4\pi)^2} \left( \frac{g_Z m_Z}{2} \right)^2 \sum_{k=1}^2 \sum_{l=3}^4 (A_{k,l-2})^2 \\ & \times \dot{B}_0(m_{A^0}^2, m_{H_k^0}^2, m_{H_l^0}^2) \\ & - \frac{1}{(4\pi)^2} 2 \left( \frac{g m_W}{2} \right)^2 \dot{B}_0(m_{A^0}^2, m_{H^+}^2, m_{W^+}^2), \end{aligned} \quad (C6)$$

$$\begin{aligned} \delta Z_{33}^{H,Z} = & \frac{1}{(4\pi)^2} \frac{g_Z^2}{4} \sum_{k=1}^2 (R_{1k}(\alpha - \beta))^2 \\ & \times [\dot{B}_0(m_{A^0}^2, m_{H_k^0}^2, m_Z^2)(2m_{A^0}^2 + 2m_{H_k^0}^2 - m_Z^2) \\ & + 2B_0(m_{A^0}^2, m_{H^0}^2, m_Z^2)], \end{aligned} \quad (C7)$$

$$\begin{aligned} \delta Z_{33}^{H,W} = & \frac{1}{(4\pi)^2} 2 \frac{g^2}{4} [\dot{B}_0(m_{A^0}^2, m_{H^+}^2, m_W^2)(2m_{A^0}^2 + 2m_{H^+}^2 - m_W^2) \\ & + 2B_0(m_{A^0}^2, m_{H^+}^2, m_W^2)]. \end{aligned} \quad (C8)$$

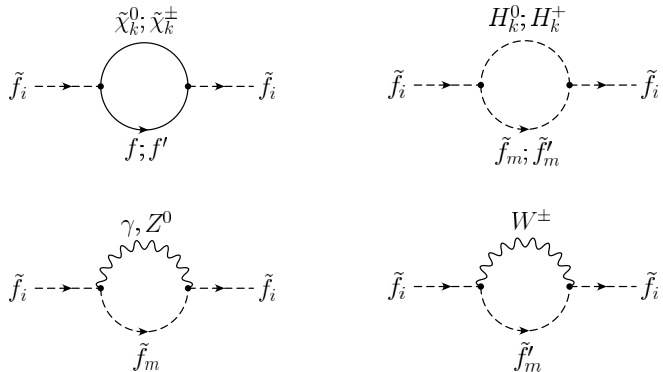


FIG. 14. Diagonal sfermion self-energies.

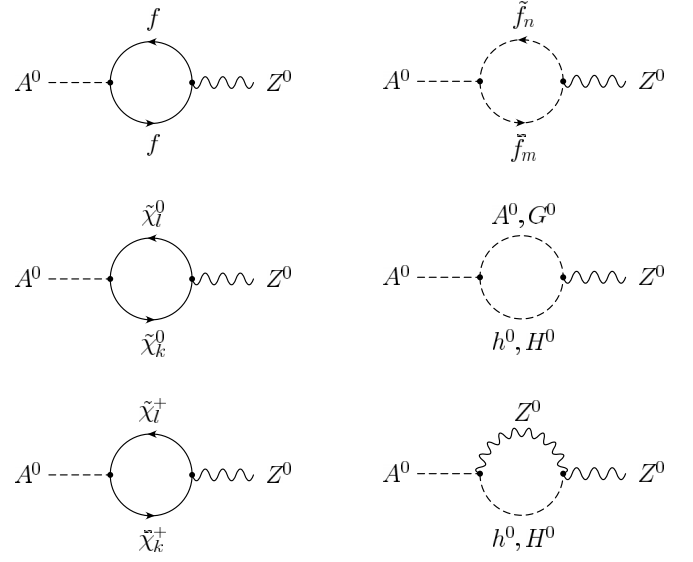


FIG. 15. AZ-mixing self-energies.

## 2. Sfermion part

$$\begin{aligned} \delta Z_{ii}^{\tilde{f},\tilde{\chi}} = & \frac{1}{(4\pi)^2} \sum_{k=1}^4 [((a_{ik}^{\tilde{f}})^2 + (b_{ik}^{\tilde{f}})^2) \cdot ((m_{\tilde{\chi}_k^0}^2 + m_{\tilde{f}}^2 - m_{\tilde{f}_i}^2) \\ & \times \dot{B}_0 - B_0) + 4m_{\tilde{\chi}_k^0} m_{\tilde{f}} a_{ik}^{\tilde{f}} b_{ik}^{\tilde{f}} \dot{B}_0] (m_{\tilde{f}_i}^2, m_{\tilde{\chi}_k^0}^2, m_{\tilde{f}}^2) \\ & + \frac{1}{(4\pi)^2} \sum_{k=1}^2 [((k_{ik}^{\tilde{f}})^2 + (l_{ik}^{\tilde{f}})^2) \cdot ((m_{\tilde{\chi}_k^+}^2 + m_{\tilde{f}'}^2 - m_{\tilde{f}_i}^2) \\ & \times \dot{B}_0 - B_0) + 4m_{\tilde{\chi}_k^+} m_{\tilde{f}'} k_{ik}^{\tilde{f}} l_{ik}^{\tilde{f}} \dot{B}_0] (m_{\tilde{f}_i}^2, m_{\tilde{\chi}_k^+}^2, m_{\tilde{f}'}^2), \end{aligned} \quad (C9)$$

$$\begin{aligned} \delta Z_{ii}^{\tilde{f},H} = & -\frac{1}{(4\pi)^2} \sum_{k=1}^4 \sum_{m=1}^2 G_{mik}^{\tilde{f}} G_{imk}^{\tilde{f}} \dot{B}_0(m_{\tilde{f}_i}^2, m_{\tilde{f}_m}^2, m_{H_k^0}^2) \\ & - \frac{1}{(4\pi)^2} \sum_{k=1}^2 \sum_{m=1}^2 G_{mik}^{\tilde{f}'\tilde{f}} G_{imk}^{\tilde{f}'\tilde{f}} \dot{B}_0(m_{\tilde{f}_i}^2, m_{\tilde{f}_m}^2, m_{H_k^+}^2), \end{aligned} \quad (C10)$$

$$\delta Z_{ii}^{\tilde{f},\gamma} = \frac{1}{(4\pi)^2} (e_0 e_f)^2 [2B_0 + (4m_{\tilde{f}_i}^2 - \lambda^2) \dot{B}_0] (m_{\tilde{f}_i}^2, m_{\tilde{f}_i}^2, \lambda^2), \quad (C11)$$

$$\begin{aligned} \delta Z_{ii}^{\tilde{f},Z} = & \frac{1}{(4\pi)^2} g_Z^2 \sum_{m=1}^2 (z_{im}^{\tilde{f}})^2 [2B_0 + (2m_{\tilde{f}_i}^2 + 2m_{\tilde{f}_m}^2 - m_Z^2) \dot{B}_0] \\ & (m_{\tilde{f}_i}^2, m_{\tilde{f}_m}^2, m_Z^2), \end{aligned} \quad (C12)$$

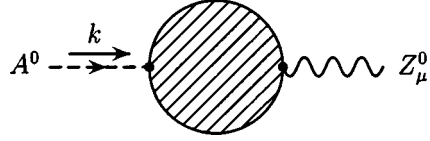
$$\begin{aligned} \delta Z_{ii}^{\tilde{f},W} = & \frac{1}{(4\pi)^2} \frac{g^2}{2} \sum_{m=1}^2 (R_{i1}^{\tilde{f}} R_{m1}^{\tilde{f}'})^2 \\ & \times [2B_0 + (2m_{\tilde{f}_i}^2 + 2m_{\tilde{f}_m}^2 - m_W^2) \dot{B}_0] (m_{\tilde{f}_i}^2, m_{\tilde{f}_m}^2, m_W^2). \end{aligned} \quad (C13)$$

## APPENDIX D: SELF-ENERGIES AND COUNTERTERMS

Here we give the explicit form of the self-energies needed for the computation of various counterterms for the one-loop width  $A^0 \rightarrow \tilde{f}_1 \tilde{f}_2$ .

## 1. AZ mixing

The scalar-vector mixing self-energy,  $\Pi_{AZ}(k^2)$ , is defined by the two-point function



$$\mathcal{M} = -i k^\mu \Pi_{AZ}(k^2) \epsilon_\mu^*(k).$$

The single contributions from the particles  $x$  are denoted by the superscript  $x$  in  $\Pi_{AZ}^x$  (see Fig. 15):

$$\Pi_{AZ}^f = -\frac{i}{(4\pi)^2} m_Z \sin 2\beta \sum_f N_C^f I_f^{3L} h_f^2 B_0(m_{A^0}^2, m_f^2, m_f^2), \quad (\text{D1})$$

$$\Pi_{AZ}^{\tilde{\chi}_l^0} = \frac{i}{(4\pi)^2} 2g g_Z \sum_{k,l=1}^4 F_{kl3}^0 O_{lk}^{\prime nL} \times [m_{\tilde{\chi}_l^0} B_0 + (m_{\tilde{\chi}_l^0} - m_{\tilde{\chi}_k^0}) B_1](m_{A^0}^2, m_{\tilde{\chi}_l^0}^2, m_{\tilde{\chi}_k^0}^2), \quad (\text{D2})$$

$$\Pi_{AZ}^{\tilde{\chi}_l^\pm} = \frac{i}{(4\pi)^2} 2g g_Z \sum_{k,l=1}^2 [(F_{kl3}^+ O_{lk}^{\prime L} - F_{lk3}^+ O_{lk}^{\prime R}) m_{\tilde{\chi}_l^\pm} (B_0 + B_1) + (F_{kl3}^+ O_{lk}^{\prime R} - F_{lk3}^+ O_{lk}^{\prime L}) m_{\tilde{\chi}_k^\pm} B_1](m_{A^0}^2, m_{\tilde{\chi}_l^\pm}^2, m_{\tilde{\chi}_k^\pm}^2), \quad (\text{D3})$$

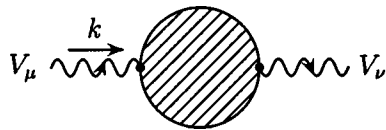
$$\Pi_{AZ}^{\tilde{f}} = -\frac{1}{(4\pi)^2} 2g g_Z \sum_f N_C^f z_{21}^{\tilde{f}} G_{123}^{\tilde{f}} \times (B_0 + 2B_1)(m_{A^0}^2, m_{\tilde{f}_1}^2, m_{\tilde{f}_2}^2), \quad (\text{D4})$$

$$\Pi_{AZ}^H = \frac{i}{(4\pi)^2} \frac{g_Z^2 m_Z}{4} \sum_{k=1}^2 \sum_{l=3}^4 A_{k,l-2} R_{k,l-2} (\beta - \alpha) \times (B_0 + 2B_1)(m_{A^0}^2, m_{H_l^0}^2, m_{H_k^0}^2), \quad (\text{D5})$$

$$\Pi_{AZ}^Z = \frac{i}{(4\pi)^2} \frac{g_Z^2 m_Z}{4} \sin(2\alpha - 2\beta) \times \sum_{k=1}^2 (-1)^k (B_0 - B_1)(m_{A^0}^2, m_{H_k^0}^2, m_Z^2). \quad (\text{D6})$$

2.  $W^+$  self-energies

For the calculation of the mass counterterm of a gauge boson  $V(V=W^\pm, Z^0)$ ,  $\delta m_V^2 = \mathfrak{A} \Pi_{VV}^T(m_V^2)$ , we need the transverse part of the vector self-energy  $\Pi_{VV}^T(k^2)$  (Fig. 16) from

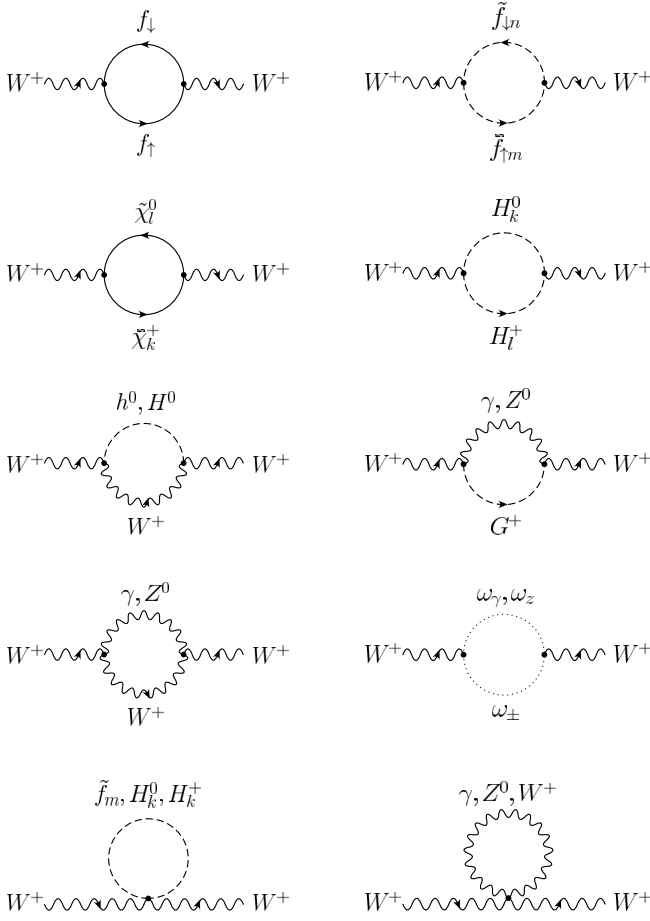
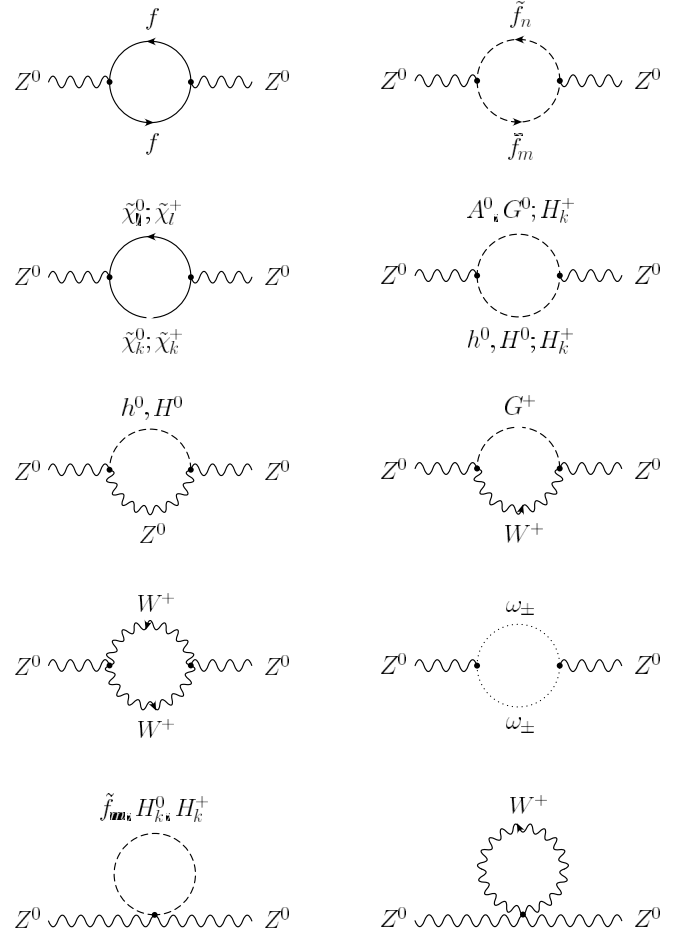


$$\mathcal{M} = -i \epsilon_\mu(k) (g^{\mu\nu} \Pi_{VV}^T(k^2) + k^\mu k^\nu \Pi_{VV}^B(k^2)) \epsilon_\nu^*(k). \quad (\text{D7})$$

$$\left( \frac{\delta m_W}{m_W} \right)^{ff} = -\frac{1}{(4\pi)^2} \sum_{\text{gen.}} N_C^f \left[ h_{f_\uparrow}^2 \sin^2 \beta \frac{A_0(m_{f_\uparrow}^2)}{m_{f_\uparrow}^2} + h_{f_\downarrow}^2 \cos^2 \beta B_0(m_W^2, m_{f_\downarrow}^2, m_{f_\uparrow}^2) - \frac{g^2}{m_W^2} B_{00}(m_W^2, m_{f_\downarrow}^2, m_{f_\uparrow}^2) + \frac{g^2}{2} B_1(m_W^2, m_{f_\downarrow}^2, m_{f_\uparrow}^2) \right], \quad (\text{D8})$$

$$\left( \frac{\delta m_W}{m_W} \right)^{\tilde{f}\tilde{f}} = -\frac{1}{(4\pi)^2} \frac{g^2}{m_W^2} \sum_{\text{gen.}} N_C^f \sum_{m,n=1}^2 (R_{m1}^{\tilde{f}} R_{n1}^{\tilde{f}})^2 B_{00}(m_W^2, m_{\tilde{f}_m}^2, m_{\tilde{f}_n}^2). \quad (\text{D9})$$

Here  $f_\uparrow$  and  $f_\downarrow$  denote up- and down-type (s)fermions of all three generations, respectively.


 FIG. 16.  $W^+$  self-energies.

 FIG. 17.  $Z^0$  self-energies.

$$\left(\frac{\delta m_W}{m_W}\right)^{\tilde{f}} = \frac{1}{(4\pi)^2} \frac{g^2}{4m_W^2} \sum_{\text{gen.}} N_C^f \times \sum_{m=1}^2 (R_{m1}^{\tilde{f}})^2 A_0(m_{f_m}^2) \quad (\text{D10})$$

$$\left(\frac{\delta m_W}{m_W}\right)^{\tilde{\chi}} = \frac{1}{(4\pi)^2} \frac{g^2}{m_W^2} \sum_{k=1}^2 \sum_{l=1}^4 [2O_{lk}^L O_{lk}^R m_{\chi_k^+}^2 m_{\chi_l^0}^2 B_0 - ((O_{lk}^L)^2 + (O_{lk}^R)^2)(m_W^2 B_1 + m_{\chi_l^0}^2 B_0 + A_0(m_{\chi_k^+}^2) - 2B_{00})] (m_W^2, m_{\chi_l^0}^2, m_{\chi_k^+}^2) \quad (\text{D11})$$

$$\left(\frac{\delta m_W}{m_W}\right)^{HH} = -\frac{1}{(4\pi)^2} \frac{g^2}{2m_W^2} \left[ \sum_{k,l=1}^2 (R_{lk}(\alpha - \beta))^2 \times B_{00}(m_W^2, m_{H_l^+}^2, m_{H_k^0}^2) + B_{00}(m_W^2, m_{H^+}^2, m_{A^0}^2) + B_{00}(m_W^2, m_{G^+}^2, m_{G^0}^2) \right] \quad (\text{D12})$$

$$\left(\frac{\delta m_W}{m_W}\right)^H = \frac{1}{(4\pi)^2} \frac{g^2}{8m_W^2} \left( \sum_{k=1}^4 A_0(m_{H_k^0}^2) + 2 \sum_{k=1}^2 A_0(m_{H_k^+}^2) \right) \quad (\text{D13})$$

$$\left(\frac{\delta m_W}{m_W}\right)^{VS} = \frac{1}{(4\pi)^2} \frac{g^2}{2} \left[ \sum_{k=1}^2 (R_{2k}(\alpha - \beta))^2 \times B_0(m_W^2, m_{H_k^0}^2, m_W^2) + s_W^2 B_0(m_W^2, m_W^2, \lambda^2) + s_W^2 t_W^2 B_0(m_W^2, m_W^2, m_Z^2) \right] \quad (\text{D14})$$

$$\left(\frac{\delta m_W}{m_W}\right)^{VV+V+\text{ghost}} = -\frac{1}{(4\pi)^2} \frac{g^2}{2m_W^2} \times [s_W^2 (8B_{00} + 7m_W^2 B_0 + 2m_W^2 B_1)(m_W^2, m_W^2, \lambda^2) + c_W^2 (8B_{00} + 7m_W^2 B_0 + 2m_W^2 B_1)(m_W^2, m_W^2, m_Z^2) - s_W^2 A_0(\lambda^2) - c_W^2 A_0(m_Z^2) - 3A_0(m_W^2)]. \quad (\text{D15})$$



### 3. $Z^0$ self-energies

According to Eq. (D7) the mass counterterm contributions to the gauge boson  $Z^0$  are (see Fig. 17)

$$\begin{aligned} \left(\frac{\delta m_Z}{m_Z}\right)^{ff} &= \frac{1}{(4\pi)^2} \frac{g_Z^2}{m_Z^2} \sum_f N_C^f [2C_L^f C_R^f m_f^2 B_0 \\ &\quad - [(C_L^f)^2 + (C_R^f)^2] (A_0(m_f^2) + m_f^2 B_0 \\ &\quad - 2B_{00} + m_Z^2 B_1)] (m_Z^2, m_f^2, m_f^2), \end{aligned} \quad (\text{D16})$$

$$\begin{aligned} \left(\frac{\delta m_Z}{m_Z}\right)^{\tilde{f}\tilde{f}} &= -\frac{1}{(4\pi)^2} \frac{2g g_Z^2}{m_Z^2} \sum_f N_C^f \sum_{m,n=1}^2 (z_{mn}^{\tilde{f}})^2 \\ &\quad \times B_{00}(m_Z^2, m_{\tilde{f}_m}^2, m_{\tilde{f}_n}^2), \end{aligned} \quad (\text{D17})$$

$$\begin{aligned} \left(\frac{\delta m_Z}{m_Z}\right)^{\tilde{f}} &= \frac{1}{(4\pi)^2} \frac{g_Z^2}{m_Z^2} \sum_f N_C^f \sum_{m=1}^2 [(C_L^f R_{m1}^{\tilde{f}})^2 \\ &\quad + (C_R^f R_{m2}^{\tilde{f}})^2] A_0(m_{\tilde{f}_m}^2), \end{aligned} \quad (\text{D18})$$

$$\begin{aligned} \left(\frac{\delta m_Z}{m_Z}\right)^{\tilde{\chi}^0} &= -\frac{1}{(4\pi)^2} \frac{g_Z^2}{m_Z^2} \sum_{k,l=1}^4 (O_{kl}^{\tilde{\chi}^0})^2 \\ &\quad \times [(m_{\tilde{\chi}_k^0}^2 + m_{\tilde{\chi}_l^0}^2) m_{\tilde{\chi}_l^0}^2 B_0 + m_Z^2 B_1 \\ &\quad + A_0(m_{\tilde{\chi}_k^0}^2) - 2B_{00}] (m_Z^2, m_{\tilde{\chi}_k^0}^2, m_{\tilde{\chi}_l^0}^2), \end{aligned} \quad (\text{D19})$$

$$\begin{aligned} \left(\frac{\delta m_Z}{m_Z}\right)^{\tilde{\chi}^+} &= \frac{1}{(4\pi)^2} \frac{g_Z^2}{m_Z^2} \sum_{k,l=1}^2 [2O_{kl}^{\prime L} O_{kl}^{\prime R} m_{\tilde{\chi}_k^+}^2 + m_{\tilde{\chi}_l^+}^2 B_0 \\ &\quad - [(O_{kl}^{\prime L})^2 + (O_{kl}^{\prime R})^2] [m_Z^2 B_1 + m_{\tilde{\chi}_k^+}^2 B_0 \\ &\quad + A_0(m_{\tilde{\chi}_k^+}^2) - 2B_{00}]] (m_Z^2, m_{\tilde{\chi}_k^+}^2, m_{\tilde{\chi}_l^+}^2), \end{aligned} \quad (\text{D20})$$

$$\begin{aligned} \left(\frac{\delta m_Z}{m_Z}\right)^{HH} &= -\frac{1}{(4\pi)^2} \frac{g_Z^2}{2m_Z^2} \left[ \sum_{k=1}^2 \sum_{l=3}^4 [R_{k,l-2}(\beta-\alpha)]^2 \right. \\ &\quad \times B_{00}(m_Z^2, m_{H_k^0}^2, m_{H_l^0}^2) \\ &\quad \left. + \cos^2(2\theta_W) \sum_{k=1}^2 B_{00}(m_Z^2, m_{H_k^+}^2, m_{H_k^+}^2) \right], \end{aligned} \quad (\text{D21})$$

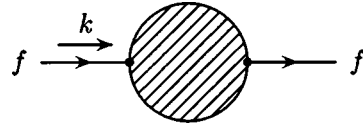
$$\begin{aligned} \left(\frac{\delta m_Z}{m_Z}\right)^H &= \frac{1}{(4\pi)^2} \frac{g_Z^2}{8m_Z^2} \left[ \sum_{k=1}^4 A_0(m_{H_k^0}^2) \right. \\ &\quad \left. + 2\cos^2(2\theta_W) \sum_{k=1}^2 A_0(m_{H_k^+}^2) \right], \end{aligned} \quad (\text{D22})$$

$$\begin{aligned} \left(\frac{\delta m_Z}{m_Z}\right)^{VS} &= \frac{1}{(4\pi)^2} \left( \frac{g_Z^2}{2} \sin^2(\alpha-\beta) B_0(m_Z^2, m_{h^0}^2, m_Z^2) \right. \\ &\quad + \frac{g_Z^2}{2} \cos^2(\alpha-\beta) B_0(m_Z^2, m_{H^0}^2, m_Z^2) \\ &\quad \left. + g^2 s_W^4 B_0(m_Z^2, m_W^2, m_{G^+}^2) \right), \end{aligned} \quad (\text{D23})$$

$$\begin{aligned} \left(\frac{\delta m_Z}{m_Z}\right)^{WW+W+\text{ghost}} &= -\frac{1}{(4\pi)^2} \frac{g^2 c_W^2}{m_Z^2} \left[ 4B_{00} + m_W^2 B_0 + \frac{5}{2} m_Z^2 B_0 \right. \\ &\quad \left. + m_Z^2 B_1 - 2A_0(m_W^2) \right] (m_Z^2, m_W^2, m_W^2). \end{aligned} \quad (\text{D24})$$

### 4. Fermion self-energies

In our notation, the fermion self-energy (Fig. 18) is defined by



$\mathcal{M} = i \bar{u}(k) \Pi(k) u(k)$

with

$$\Pi(k) = \not{k} P_L \Pi^L(k) + \not{k} P_R \Pi^R(k) + \Pi^{SL}(k) P_L + \Pi^{SR}(k) P_R. \quad (\text{D25})$$

Thus the counterterm for quarks and leptons is given by

$$\delta m_f = \frac{1}{2} \Re \{ m_f [\Pi^L(m_f) + \Pi^R(m_f)] + \Pi^{SL}(m_f) + \Pi^{SR}(m_f) \}. \quad (\text{D26})$$

Note that for quarks and leptons (unlike charginos), the left- and right-handed scalar parts of  $\Pi(k)$  are equal,  $\Pi^{SL}(k) = \Pi^{SR}(k)$ . The single contributions to  $\delta m_f$  are as follows:

$$\left(\frac{\delta m_f}{m_f}\right)^{fH_k^0} = \frac{1}{(4\pi)^2} \left[ \sum_{k=1}^2 (s_k^f)^2 (B_0 - B_1) + \sum_{k=3}^4 (s_k^f)^2 (B_0 + B_1) \right] (m_{\tilde{f}}^2, m_{\tilde{f}}^2, m_{H_k^0}^2), \quad (\text{D27})$$

$$\left(\frac{\delta m_f}{m_f}\right)^{f'H_k^+} = -\frac{1}{(4\pi)^2} \sum_{k=1}^2 \left[ \frac{1}{2} [(y_k^f)^2 + (y_k^{f'})^2] B_1 - \frac{m_{f'}}{m_f} y_k^f y_k^{f'} B_0 \right] (m_f^2, m_{f'}^2, m_{H_k^+}^2), \quad (\text{D28})$$

$$\left(\frac{\delta m_f}{m_f}\right)^{\tilde{f}\tilde{\chi}^0} = -\frac{1}{(4\pi)^2} \sum_{m=1}^2 \sum_{k=1}^4 \left[ \frac{1}{2} [(a_{mk}^{\tilde{f}})^2 + (b_{mk}^{\tilde{f}})^2] B_1 - \frac{m_{\tilde{\chi}_k^0}}{m_f} a_{mk}^{\tilde{f}} b_{mk}^{\tilde{f}} B_0 \right] (m_f^2, m_{\tilde{\chi}_k^0}^2, m_{\tilde{f}_m}^2), \quad (\text{D29})$$

$$\left(\frac{\delta m_f}{m_f}\right)^{\tilde{f}'\tilde{\chi}^+} = -\frac{1}{(4\pi)^2} \sum_{m=1}^2 \sum_{k=1}^2 \left[ \frac{1}{2} [(k_{mk}^{\tilde{f}'})^2 + (l_{mk}^{\tilde{f}'})^2] B_1 - \frac{m_{\tilde{\chi}_k^+}}{m_f} k_{mk}^{\tilde{f}'} l_{mk}^{\tilde{f}'} B_0 \right] (m_f^2, m_{\tilde{\chi}_k^+}^2, m_{\tilde{f}'_m}^2), \quad (\text{D30})$$

$$\left(\frac{\delta m_f}{m_f}\right)^{f\gamma} = -\frac{1}{(4\pi)^2} 2(e_0 e_f)^2 (B_0 - B_1) (m_f^2, \lambda^2, m_f^2), \quad (\text{D31})$$

$$\left(\frac{\delta m_f}{m_f}\right)^{fZ^0} = -\frac{1}{(4\pi)^2} g_Z^2 \{ [(C_L^f)^2 + (C_R^f)^2] B_1 + 4C_L^f C_R^f B_0 \} (m_f^2, m_f^2, m_Z^2), \quad (\text{D32})$$

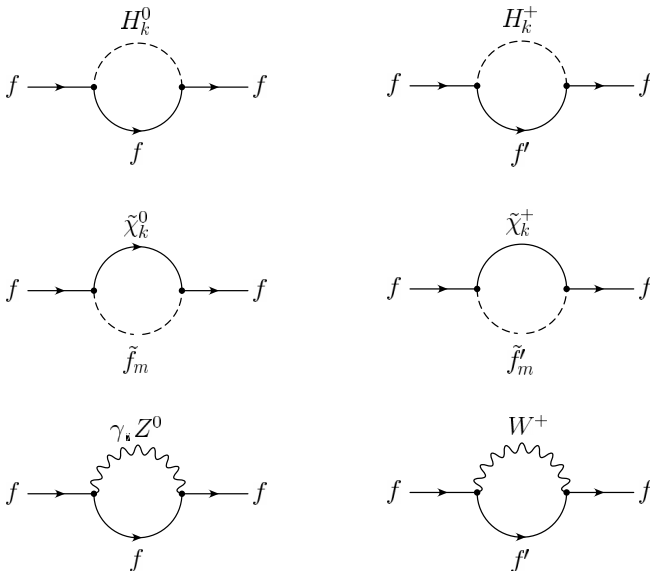


FIG. 18. Fermion self-energies.

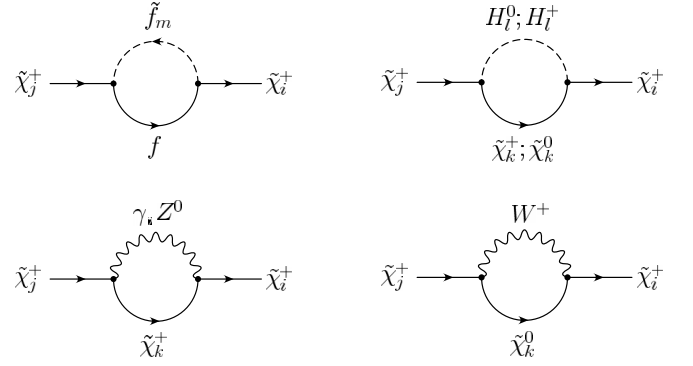


FIG. 19. Chargino self-energies.

$$\left(\frac{\delta m_f}{m_f}\right)^{f'W^+} = -\frac{1}{(4\pi)^2} \frac{g^2}{2} B_1 (m_f^2, m_{f'}^2, m_W^2). \quad (\text{D33})$$

### 5. Chargino self-energies

Since the Higgsino mass parameter  $\mu$  is fixed in the chargino sector, the counterterm  $\delta\mu$  reads [20,21]

$$\delta\mu = \delta X_{22} = \frac{1}{2} \sum_{i,j=1}^2 U_{i2} V_{j2} (\Pi_{ji}^L m_{\tilde{\chi}_i^+} + \Pi_{ij}^R m_{\tilde{\chi}_j^+} + \Pi_{ij}^{SL} + \Pi_{ji}^{SR}) \quad (\text{D34})$$

with the chargino self-energies  $\Pi_{ij} = \Pi_{ij}(m_{\tilde{\chi}_j^+}^2)$  (see Fig. 19).

$U$  and  $V$  are two real  $2 \times 2$  matrices which diagonalize the chargino mass matrix,

$$UXV^T = M_D = \begin{pmatrix} m_{\tilde{\chi}_1^+} & 0 \\ 0 & m_{\tilde{\chi}_2^+} \end{pmatrix}.$$

The single left- and right-handed parts of  $\Pi_{ij}$  can be found by comparing the coefficients according to Eq. (D25).

For the fermion-sfermion contribution,

$$\begin{aligned} \Pi_{ij}^{L,f}(k^2) &= -\frac{1}{(4\pi)^2} \sum_f N_C^f \sum_{m=1}^2 [k_{mi}^{\tilde{f}} l_{mj}^{\tilde{f}} B_1(k^2, m_{\tilde{f}_1}^2, m_{\tilde{f}_{1m}}^2) \\ &\quad + l_{mi}^{\tilde{f}} l_{mj}^{\tilde{f}} B_1(k^2, m_{\tilde{f}_1}^2, m_{\tilde{f}_{1m}}^2)], \\ \Pi_{ij}^{R,f}(k^2) &= -\frac{1}{(4\pi)^2} \sum_f N_C^f \sum_{m=1}^2 [l_{mi}^{\tilde{f}} l_{mj}^{\tilde{f}} B_1(k^2, m_{\tilde{f}_1}^2, m_{\tilde{f}_{1m}}^2) \\ &\quad + k_{mi}^{\tilde{f}} k_{mj}^{\tilde{f}} B_1(k^2, m_{\tilde{f}_1}^2, m_{\tilde{f}_{1m}}^2)], \\ \Pi_{ij}^{SL,f}(k^2) &= \frac{1}{(4\pi)^2} \sum_f N_C^f \sum_{m=1}^2 [m_{\tilde{f}_1} l_{mi}^{\tilde{f}} k_{mj}^{\tilde{f}} B_0(k^2, m_{\tilde{f}_1}^2, m_{\tilde{f}_{1m}}^2) \\ &\quad + m_{\tilde{f}_1} k_{mi}^{\tilde{f}} l_{mj}^{\tilde{f}} B_0(k^2, m_{\tilde{f}_1}^2, m_{\tilde{f}_{1m}}^2)], \end{aligned}$$

$$\begin{aligned} \Pi_{ij}^{SR,f}(k^2) = & \frac{1}{(4\pi)^2} \sum_f N_C^f \sum_{m=1}^2 [m_{f_1} \tilde{k}_{mi}^{\tilde{f}_1} \tilde{l}_{mj}^{\tilde{f}_1} B_0(k^2, m_{f_1}^2, m_{\tilde{f}_1 m}^2) \\ & + m_{f_1} \tilde{l}_{mi}^{\tilde{f}_1} \tilde{k}_{mj}^{\tilde{f}_1} B_0(k^2, m_{f_1}^2, m_{\tilde{f}_1 m}^2)]. \end{aligned} \quad (D35)$$

For the Higgs-boson-gaugino contribution,

$$\begin{aligned} \Pi_{ij}^{H_l^0}(k) = & -\frac{1}{(4\pi)^2} g^2 \sum_{k=1}^2 \left[ \mathbf{k} \sum_{l=1}^4 (F_{ikl}^+ F_{jkl}^+ P_L + F_{kil}^+ F_{kjl}^+ P_R) B_1 \right. \\ & - m_{\tilde{\chi}_k^+} \sum_{l=1}^2 (F_{kil}^+ F_{jkl}^+ P_L + F_{ikl}^+ F_{kjl}^+ P_R) B_0 \\ & \left. + m_{\tilde{\chi}_k^+} \sum_{l=3}^4 (F_{kil}^+ F_{jkl}^+ P_L + F_{ikl}^+ F_{kjl}^+ P_R) B_0 \right] (k^2, m_{\tilde{\chi}_k^+}^2, m_{H_l^0}^2), \end{aligned} \quad (D36)$$

$$\begin{aligned} \Pi_{ij}^{H_l^+}(k) = & -\frac{1}{(4\pi)^2} g^2 \sum_{k=1}^4 \sum_{l=1}^2 [\mathbf{k} (F_{ikl}^R F_{jkl}^R P_L + F_{ikl}^L F_{jkl}^L P_R) B_1 \\ & - m_{\tilde{\chi}_k^0} (F_{ikl}^L F_{jkl}^R P_L + F_{ikl}^R F_{jkl}^L P_R) B_0] (k^2, m_{\tilde{\chi}_k^0}^2, m_{H_l^+}^2). \end{aligned} \quad (D37)$$

For the vector-gaugino contribution,

$$\Pi_{ij}^\gamma(k) = -\frac{1}{(4\pi)^2} 2e^2 \delta_{ij} [\mathbf{k} B_1 + 2m_{\tilde{\chi}_j^+} B_0] (k^2, m_{\tilde{\chi}_j^+}^2, \lambda^2), \quad (D38)$$

$$\begin{aligned} \Pi_{ij}^{Z^0}(k) = & -\frac{1}{(4\pi)^2} 2g_Z^2 \sum_{k=1}^2 [\mathbf{k} (O_{ik}^{\prime L} O_{kj}^{\prime L} P_L + O_{ik}^{\prime R} O_{kj}^{\prime R} P_R) B_1 \\ & + 2m_{\tilde{\chi}_k^+} (O_{ik}^{\prime R} O_{kj}^{\prime L} P_L + O_{ik}^{\prime L} O_{kj}^{\prime R} P_R) B_0] (k^2, m_{\tilde{\chi}_k^+}^2, m_Z^2), \end{aligned} \quad (D39)$$

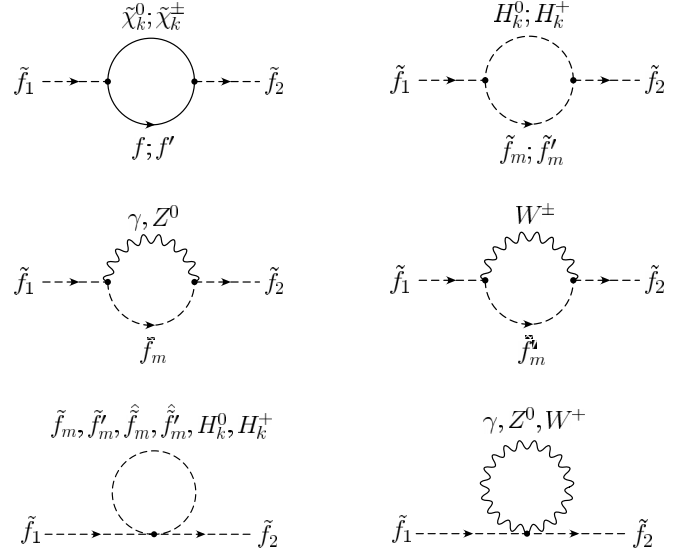


FIG. 20. Off-diagonal sfermion self-energies.

$$\begin{aligned} \Pi_{ij}^{W^+}(k) = & -\frac{1}{(4\pi)^2} 2g^2 \sum_{k=1}^4 [\mathbf{k} (O_{ki}^L O_{kj}^L P_L + O_{ki}^R O_{kj}^R P_R) B_1 \\ & + 2m_{\tilde{\chi}_k^0} (O_{ki}^R O_{kj}^L P_L + O_{ki}^L O_{kj}^R P_R) B_0] (k^2, m_{\tilde{\chi}_k^0}^2, m_W^2). \end{aligned} \quad (D40)$$

## 6. Sfermion self-energies

For the fixing of the sfermion mixing angle  $\theta_{\tilde{f}}$  we need the off-diagonal elements of the sfermion self-energies (Fig. 20),  $\Pi_{ij}^{\tilde{f}} = \Pi_{ij}^{\tilde{f}}(m_{\tilde{f}_j}^2)$ . In the following,  $Y_{L/R}^f$  denotes the weak hypercharge,  $Y_{L/R}^f = 2(I_f^{3L/R} - e_f)$ . The short forms for various products of sfermion rotation matrices can be found in Appendix B. Additionally, we use the abbreviation  $R_{ijkl}^{\tilde{f}\tilde{f}D} = R_{i1}^{\tilde{f}} R_{j1}^{\tilde{f}} R_{k2}^{\tilde{f}} R_{l2}^{\tilde{f}}$ .

$$\begin{aligned} \Pi_{ij}^{\tilde{f}, \tilde{\chi}} = & -\frac{1}{(4\pi)^2} \sum_{k=1}^4 [(a_{ik}^{\tilde{f}} a_{jk}^{\tilde{f}} + b_{ik}^{\tilde{f}} b_{jk}^{\tilde{f}}) \cdot (A_0(m_{\tilde{\chi}_k^0}^2) + A_0(m_{f'}^2) + (m_{\tilde{\chi}_k^0}^2 + m_{f'}^2 - m_{\tilde{f}_j}^2) B_0) \\ & + (a_{ik}^{\tilde{f}} b_{jk}^{\tilde{f}} + b_{ik}^{\tilde{f}} a_{jk}^{\tilde{f}}) \cdot 2m_{\tilde{\chi}_k^0} m_{f'} B_0] (m_{\tilde{f}_j}^2, m_{\tilde{\chi}_k^0}^2, m_{f'}^2) \\ & - \frac{1}{(4\pi)^2} \sum_{k=1}^2 [(k_{ik}^{\tilde{f}} k_{jk}^{\tilde{f}} + l_{ik}^{\tilde{f}} l_{jk}^{\tilde{f}}) \cdot (A_0(m_{\tilde{\chi}_k^+}^2) + A_0(m_{f'}^2) + (m_{\tilde{\chi}_k^+}^2 + m_{f'}^2 - m_{\tilde{f}_j}^2) B_0) \\ & + (k_{ik}^{\tilde{f}} l_{jk}^{\tilde{f}} + l_{ik}^{\tilde{f}} k_{jk}^{\tilde{f}}) \cdot 2m_{\tilde{\chi}_k^+} m_{f'} B_0] (m_{\tilde{f}_j}^2, m_{\tilde{\chi}_k^+}^2, m_{f'}^2), \end{aligned} \quad (D41)$$

$$\Pi_{ij}^{\tilde{f}, H} = \frac{1}{(4\pi)^2} \sum_{k=1}^4 \sum_{m=1}^2 G_{mik}^{\tilde{f}} G_{jmk}^{\tilde{f}} B_0(m_{\tilde{f}_j}^2, m_{\tilde{f}_m}^2, m_{H_k^0}^2) + \frac{1}{(4\pi)^2} \sum_{k=1}^2 \sum_{m=1}^2 G_{mik}^{\tilde{f}\tilde{f}'} G_{jmk}^{\tilde{f}\tilde{f}'} B_0(m_{\tilde{f}_j}^2, m_{\tilde{f}_m}^2, m_{H_k^+}^2), \quad (D42)$$

$$\Pi_{ij}^{\tilde{f},\tilde{f}} = -\frac{1}{(4\pi)^2} (e_0 e_f)^2 \delta_{ij} [2A_0(\lambda^2) - A_0(m_{\tilde{f}_i}^2) + (4m_{\tilde{f}_i}^2 - \lambda^2)B_0(m_{\tilde{f}_i}^2, m_{\tilde{f}_i}^2, \lambda^2)], \quad (\text{D43})$$

$$\Pi_{ij}^{\tilde{f},Z\tilde{f}} = -\frac{1}{(4\pi)^2} g_Z^2 \sum_{m=1}^2 z_{mi} z_{jm} \tilde{f} [2A_0(m_Z^2) - A_0(m_{\tilde{f}_m}^2) + (2m_{\tilde{f}_j}^2 + 2m_{\tilde{f}_m}^2 - m_Z^2)B_0(m_{\tilde{f}_j}^2, m_{\tilde{f}_m}^2, m_Z^2)], \quad (\text{D44})$$

$$\Pi_{ij}^{\tilde{f},W\tilde{f}'} = -\frac{1}{(4\pi)^2} \frac{g^2}{2} R_{i1}^{\tilde{f}} R_{j1}^{\tilde{f}'} \sum_{m=1}^2 (R_{m1}^{\tilde{f}'})^2 [2A_0(m_W^2) - A_0(m_{\tilde{f}'_m}^2) + (2m_{\tilde{f}_j}^2 + 2m_{\tilde{f}'_m}^2 - m_W^2)B_0(m_{\tilde{f}_j}^2, m_{\tilde{f}'_m}^2, m_W^2)], \quad (\text{D45})$$

$$\begin{aligned} \Pi_{ij}^{\tilde{f},\tilde{f}} &= \frac{1}{(4\pi)^2} h_f^2 \sum_{m=1}^2 [N_C^f (R_{jmmi}^{\tilde{f}} + R_{mijm}^{\tilde{f}}) + R_{jimmm}^{\tilde{f}} + R_{mmji}^{\tilde{f}}] A_0(m_{\tilde{f}_m}^2) \\ &+ \frac{1}{(4\pi)^2} g_Z^2 \sum_{m=1}^2 \left\{ \left[ \left( \frac{1}{4} - (2I_f^{3L} - e_f) e_f s_W^2 \right) R_{jimmm}^{\tilde{f}L} + e_f^2 s_W^2 R_{jimmm}^{\tilde{f}R} \right] (N_C^f + 1) \right. \\ &\left. + (I_f^{3L} - e_f) e_f s_W^2 [N_C^f (R_{jimm}^{\tilde{f}} + R_{mmji}^{\tilde{f}}) + R_{jmmi}^{\tilde{f}} + R_{mijm}^{\tilde{f}}] \right\} A_0(m_{\tilde{f}_m}^2), \end{aligned} \quad (\text{D46})$$

$$\begin{aligned} \Pi_{ij}^{\tilde{f},\tilde{f}'} &= \frac{1}{(4\pi)^2} \sum_{m=1}^2 (h_f^2 R_{mmji}^{\tilde{f}'D} + h_f^2 R_{jimmm}^{\tilde{f}'D}) A_0(m_{\tilde{f}'_m}^2) + \frac{1}{(4\pi)^2} \frac{g^2}{4} \\ &\times \sum_{m=1}^2 \{ N_C^f [(t_W^2 Y_L^f Y_L^{f'} - 1) R_{jimmm}^{\tilde{f}'L} + t_W^2 Y_R^f Y_R^{f'} R_{jimmm}^{\tilde{f}'R} - Y_L^f Y_R^{f'} R_{jimmm}^{\tilde{f}'D} - Y_L^{f'} Y_R^f R_{mmji}^{\tilde{f}'D}] + 2R_{jimmm}^{\tilde{f}'L} \} A_0(m_{\tilde{f}'_m}^2), \end{aligned} \quad (\text{D47})$$

$$\begin{aligned} \Pi_{ij}^{\tilde{f},\hat{\tilde{f}}} &= \frac{1}{(4\pi)^2} N_C^f \sum_{m=1}^2 \left[ h_f h_{\hat{f}} (R_{jimm}^{\hat{\tilde{f}}F} + R_{jimmm}^{\hat{\tilde{f}}F}) + \frac{g^2}{4} R_{jimmm}^{\hat{\tilde{f}}L} \right] A_0(m_{\hat{\tilde{f}}_m}^2) \\ &+ \frac{1}{(4\pi)^2} N_C^f \frac{g'^2}{4} \sum_{m=1}^2 [Y_L^f Y_L^{\hat{f}} R_{jimm}^{\hat{\tilde{f}}L} - Y_L^f Y_R^{\hat{f}} R_{jimm}^{\hat{\tilde{f}}D} - Y_L^{\hat{f}} Y_R^f R_{mmji}^{\hat{\tilde{f}}D} + Y_R^f Y_R^{\hat{f}} R_{jimm}^{\hat{\tilde{f}}R}] A_0(m_{\hat{\tilde{f}}_m}^2), \end{aligned} \quad (\text{D48})$$

$$\begin{aligned} \Pi_{ij}^{\tilde{f},\hat{\tilde{f}}'} &= -\frac{1}{(4\pi)^2} N_C^f \frac{g^2}{4} \sum_{m=1}^2 R_{jimmm}^{\hat{\tilde{f}}'L} A_0(m_{\hat{\tilde{f}}'_m}^2) \\ &+ \frac{1}{(4\pi)^2} N_C^f \frac{g'^2}{4} \sum_{m=1}^2 [Y_L^f Y_L^{\hat{f}'} R_{jimm}^{\hat{\tilde{f}}'L} - Y_L^f Y_R^{\hat{f}'} R_{jimm}^{\hat{\tilde{f}}'D} - Y_L^{\hat{f}'} Y_R^f R_{mmji}^{\hat{\tilde{f}}'D} + Y_R^f Y_R^{\hat{f}'} R_{jimm}^{\hat{\tilde{f}}'R}] A_0(m_{\hat{\tilde{f}}'_m}^2). \end{aligned} \quad (\text{D49})$$

The contributions from first and second generation sfermions,  $\tilde{F}_m$ , are given by

$$\Pi_{ij}^{\tilde{f},\tilde{F}} = \Pi_{ij}^{\tilde{f},\hat{\tilde{f}}}(\hat{f} \rightarrow F), \quad \Pi_{ij}^{\tilde{f},\hat{\tilde{F}}} = \Pi_{ij}^{\tilde{f},\hat{\tilde{f}}}(\hat{f} \rightarrow \hat{F}), \quad \Pi_{ij}^{\tilde{f},\tilde{F}'} = \Pi_{ij}^{\tilde{f},\hat{\tilde{f}}'}(\hat{f}' \rightarrow F'), \quad \Pi_{ij}^{\tilde{f},\hat{\tilde{F}}'} = \Pi_{ij}^{\tilde{f},\hat{\tilde{f}}'}(\hat{f}' \rightarrow \hat{F}'), \quad (\text{D50})$$

where the superscript  $\tilde{F}$  denotes values belonging to first and second generation scalar fermions with the same isospin as  $\tilde{f}$  (e.g.  $\tilde{F}_1 = \{\tilde{u}_1, \tilde{c}_1\}$  for the top squark case),  $\tilde{F}'$  sfermions with different isospin etc.

$$\begin{aligned} \Pi_{ij}^{\tilde{f},H} &= \frac{1}{(4\pi)^2} \frac{1}{2} \sum_{k=1}^4 [h_f^2 c_{kk}^{\tilde{f}} \delta_{ij} + g^2 e_{ij}^{\tilde{f}} (c_{kk}^{\tilde{b}} - c_{kk}^{\tilde{t}})] A_0(m_{H_k^0}^2) \\ &+ \frac{1}{(4\pi)^2} \sum_{k=1}^2 [h_f^2 d_{kk}^{\tilde{f}} R_{i1}^{\tilde{f}} R_{j1}^{\tilde{f}} + h_f^2 d_{kk}^{\tilde{f}} R_{i2}^{\tilde{f}} R_{j2}^{\tilde{f}} + g^2 f_{ij}^{\tilde{f}} (d_{kk}^{\tilde{b}} - d_{kk}^{\tilde{t}})] A_0(m_{H_k^+}^2), \end{aligned} \quad (\text{D51})$$

$$\Pi_{ij}^{\tilde{f},V} = \frac{1}{(4\pi)^2} 4(e_0 e_f)^2 \delta_{ij} A_0(\lambda^2) + \frac{1}{(4\pi)^2} 2g^2 R_{i1}^{\tilde{f}} R_{j1}^{\tilde{f}} A_0(m_w^2) + \frac{1}{(4\pi)^2} 4g_z^2 [(C_L^f)^2 R_{i1}^{\tilde{f}} R_{j1}^{\tilde{f}} + (C_R^f)^2 R_{i2}^{\tilde{f}} R_{j2}^{\tilde{f}}] A_0(m_z^2). \quad (\text{D52})$$

- [1] The LEP Collaborations ALEPH, DELPHI, L3, OPAL, and the LEP Working Group for Higgs Boson Searches “Search for the Standard Model Higgs Boson at LEP”, CERN-EP/2003-011.
- [2] J.F. Gunion and H.E. Haber, Nucl. Phys. **B272**, 1 (1986); **B402**, 567(E) (1993).
- [3] J. F. Gunion, H. E. Haber, G. L. Kane, and S. Dawson, *The Higgs Hunter’s Guide* (Addison-Wesley, Reading, MA, 1990).
- [4] H. Baer, D. Dicus, M. Drees, and X. Tata, Phys. Rev. D **36**, 1363 (1987); J.F. Gunion and H.E. Haber, Nucl. Phys. **B307**, 445 (1988); **B402**, 569(E) (1993); K. Griest and H.E. Haber, Phys. Rev. D **37**, 719 (1988).
- [5] A. Djouadi, J. Kalinowski, and P.M. Zerwas, Z. Phys. C **57**, 569 (1993); A. Djouadi, P. Janot, J. Kalinowski, and P.M. Zerwas, Phys. Lett. B **376**, 220 (1996); A. Djouadi, J. Kalinowski, P. Ohmann, and P.M. Zerwas, Z. Phys. C **74**, 93 (1997); A. Djouadi, Mod. Phys. Lett. A **14**, 359 (1999); G. Bélanger, F. Boudjema, F. Donato, R. Godbole, and S. Rosier-Lees, Nucl. Phys. **B581**, 3 (2000).
- [6] A. Bartl, K. Hidaka, Y. Kizukuri, T. Kon, and W. Majerotto, Phys. Lett. B **315**, 360 (1993); A. Djouadi, J. Kalinowski, P. Ohmann, and P.M. Zerwas, Z. Phys. C **74**, 93 (1997).
- [7] A. Bartl, H. Eberl, K. Hidaka, T. Kon, W. Majerotto, and Y. Yamada, Phys. Lett. B **378**, 167 (1996), and references therein.
- [8] A. Bartl, H. Eberl, K. Hidaka, T. Kon, W. Majerotto, and Y. Yamada, Phys. Lett. B **402**, 303 (1997).
- [9] A. Arhrib, A. Djouadi, W. Hollik, and C. Jünger, Phys. Rev. D **57**, 5860 (1998).
- [10] H. Eberl, M. Kincel, W. Majerotto, and Y. Yamada, Nucl. Phys. **B625**, 372 (2002).
- [11] R.Y. Zhang *et al.* Phys. Rev. D **65**, 075018 (2002).
- [12] C. Weber, H. Eberl, and W. Majerotto, hep-ph/0305250.
- [13] R. Hempfling, Phys. Rev. D **49**, 6168 (1994); L.J. Hall, R. Rattazzi, and U. Sarid, *ibid.* **50**, 7048 (1994); M. Carena, M. Olechowski, S. Pokorski, and C.E.M. Wagner, Nucl. Phys. **B426**, 269 (1994); D.M. Pierce, J.A. Bagger, K. Matchev, and R. Zhang, *ibid.* **B491**, 3 (1997).
- [14] H. Eberl, K. Hidaka, S. Kraml, W. Majerotto, and Y. Yamada, Phys. Rev. D **62**, 055006 (2000).
- [15] E. Braaten and J.P. Leveille, Phys. Rev. D **22**, 715 (1980); M. Drees and K. Hikasa, Phys. Lett. B **240**, 455 (1990); **262**, 497(E) (1991); A. Méndez and A. Pomarol, *ibid.* **252**, 461 (1990).
- [16] S.G. Gorishny, A.L. Kataev, S.A. Larin, and L.R. Surguladze, Mod. Phys. Lett. A **5**, 2703 (1990); Phys. Rev. D **43**, 1633 (1991); A. Djouadi, M. Spira, and P.M. Zerwas, Z. Phys. C **70**, 427 (1996); A. Djouadi, J. Kalinowski, and M. Spira, Comput. Phys. Commun. **108**, 56 (1998); M. Spira, Fortschr. Phys. **46**, 203 (1998).
- [17] M. Carena, S. Mrenna, and C.E.M. Wagner, Phys. Rev. D **60**, 075010 (1999); **62**, 055008 (2000).
- [18] P.H. Chankowski and S. Pokorski, in *Perspectives on Supersymmetry*, edited by G. L. Kane (World Scientific, Singapore, 1997), hep-ph/9707497; K.S. Babu and C. Kolda, Phys. Lett. B **451**, 77 (1999).
- [19] J. Guasch, J. Solá, and W. Hollik, Phys. Lett. B **437**, 88 (1998); H. Eberl, S. Kraml, and W. Majerotto, J. High Energy Phys. **05**, 016 (1999).
- [20] H. Eberl, M. Kincel, W. Majerotto, and Y. Yamada, Phys. Rev. D **64**, 115013 (2001).
- [21] W. Öller, H. Eberl, W. Majerotto, and C. Weber, hep-ph/0304006.
- [22] P.H. Chankowski, S. Pokorski, and J. Rosiek, Phys. Lett. B **274**, 191 (1992); Nucl. Phys. **B423**, 437 (1994); **B423**, 497 (1994); A. Dabelstein, Z. Phys. C **67**, 495 (1995); Nucl. Phys. **B456**, 25 (1995).
- [23] G. ’t Hooft and M. Veltman, Nucl. Phys. **B153**, 365 (1979); G. Passarino and M. Veltman, *ibid.* **B160**, 151 (1979).
- [24] A. Denner, Fortschr. Phys. **41**, 307 (1993).